AD-A096 682 VIRGINIA POLYTECHNIC INST AND STATE UNIV BLACKSBURG --ETC F/G 11/9
AN OVERVIEW OF THE NONEQUILIBRIUM BEHAVIOR OF POLYMER GLASSES.(U)
MAR 81 M R TANT, G L WILKES N00014-78-C-0629
UNCLASSIFIED TR-4 NL

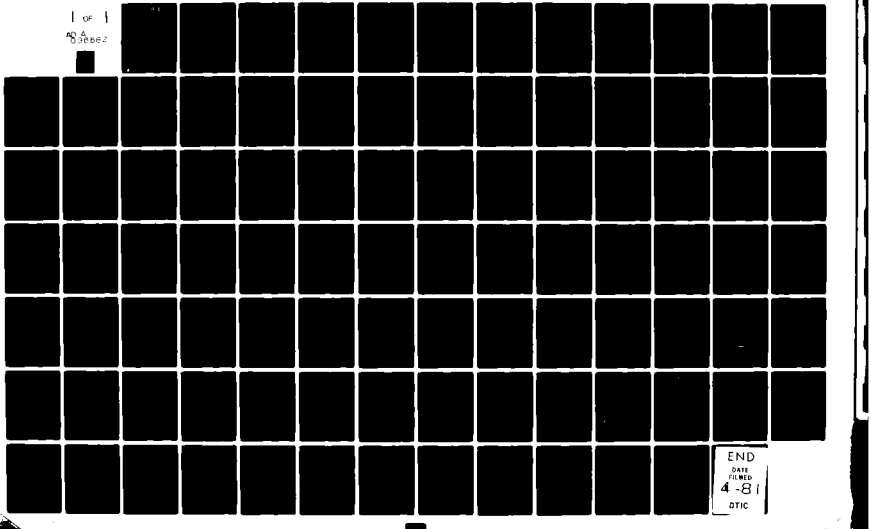

OFFICE OF NAVAL RESEARCH
Contract N00014-78-C-0629
Task No. NR 356-692

TECHNICAL REPORT NO. 4

14 TR-4

An Overview of the Nonequilibrium Behavior of Polymer Glasses

by

M. R. Tant and G. L. Wilkes

Prepared for Publication

in

Polymer Engineering and Science

Virginia Polytechnic Institute and State University
Department of Chemical Engineering
Blacksburg, Virginia

11 13 Mar 1981

12 94

SECURITY CLASSIFICATION OF THIS PAGE (When Data Entered)

REPORT DOCUMENTATION PAGE		READ INSTRUCTIONS BEFORE COMPLETING FORM
1. REPORT NUMBER: 4	2. GOVT ACCESSION NO.: AD-A096 682	3. RECIPIENT'S CATALOG NUMBER:
4. TITLE (and Subtitle): An Overview of the Nonequilibrium Behavior of Polymer Glasses		5. TYPE OF REPORT & PERIOD COVERED: Technical
		6. PERFORMING ORG. REPORT NUMBER:
7. AUTHOR(s): M. R. Tanc and G. L. Wilkes		8. CONTRACT OR GRANT NUMBER(s): N00014-78-C-0629
9. PERFORMING ORGANIZATION NAME AND ADDRESS: Virginia Polytechnic Institute & State Univ. Department of Chemical Engineering Blacksburg Virginia 24061		10. PROGRAM ELEMENT, PROJECT, TASK AREA & WORK UNIT NUMBERS: NR 356-692
11. CONTROLLING OFFICE NAME AND ADDRESS: Department of the Navy Office of Naval Reserach, Code 472 Arlington, Virginia 22217		12. REPORT DATE: March 13, 1981
		13. NUMBER OF PAGES: 91
14. MONITORING AGENCY NAME & ADDRESS(if different from Controlling Office)		15. SECURITY CLASS. (of this report): Unclassified
		15a. DECLASSIFICATION/DOWNGRADING SCHEDULE

16. DISTRIBUTION STATEMENT (of this Report)

Reproduction in whole or in part is permitted for any purpose of the United States Government.

This document has been approved for public release and sale -- its distribution is unlimited.

17. DISTRIBUTION STATEMENT (of the abstract entered in Block 20, if different from Report)

18. SUPPLEMENTARY NOTES

19. KEY WORDS (Continue on reverse side if necessary and identify by block number)

Polymer glasses
Non equilibrium glasses
Epoxy
Resins
Composites

20. ABSTRACT (Continue on reverse side if necessary and identify by block number)

An overview is given of the nonequilibrium behavior of polymeric glasses. While the emphasis is to display the significant effects of the nonequilibrium behavior on observable properties, some general basics of the glass transition behavior and nonequilibrium behavior are also presented Both molecular as well as phenomenological explanations of the nonequilibrium phenomenon are considered. The overview is not meant to be exhaustive but has the principal objective to introduce and educate the newcomer to this topic of polymer science.

DD FORM 1 JAN 73 1473 EDITION OF 1 NOV 65 IS OBSOLETE

SECURITY CLASSIFICATION OF THIS PAGE (When Data Entered)

AN OVERVIEW OF THE NONEQUILIBRIUM BEHAVIOR OF POLYMER GLASSES

ABSTRACT

An overview is given of the nonequilibrium behavior of polymeric glasses. While the emphasis is to display the significant effects of the nonequilibrium behavior on observable properties, some general basics of the glass transition behavior and nonequilibrium behavior are also presented. Both molecular as well as phenomenological explanations of the nonequilibrium phenomenon are considered. The overview is not meant to be exhaustive but has the principal objective to introduce and educate the newcomer to this topic of polymer science.

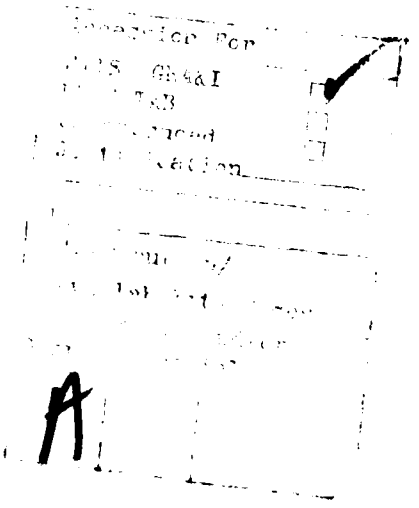

I. INTRODUCTION

During recent years there has been increased interest in the structural and property changes that occur in glassy and partially glassy polymers upon annealing below the glass transition temperature. This aging or time dependent behavior is a direct result of the nonequilibrium nature of the glassy state and has been observed to occur in many types of polymer systems containing glassy regions--purely glassy polymers, semi-crystalline polymers, polymeric network glasses, and block copolymers.[+] The importance of this phenomenon in applications stems from the simple fact that material performance must necessarily be predictable to ensure compliance with design specifications throughout the anticipated service life of the fabricated polymer product. The current fervent state of research activity in this area, as well as the appearance of review papers [1,2] and a book [3] on the subject, as well as the following proceedings from this 1980 conference, gives testimony to the importance of the nonequilibrium phenomenon in polymer glasses. Research efforts are presently being directed in two areas: (1) experimental studies of this phenomenon in various glassy polymer systems, and (2) development of a quantitative theory capable of satisfactorily predicting aging behavior for a variety of polymer materials under different conditions. Within this paper, we will consider recent and present work in both of these areas. The papers that follow will focus in more detail on several of the subject areas that will be touched upon in this review.

[+]This nonequilibrium behavior is not unique to only polymeric systems. It also can be observed in lower molecular weight glassy systems but these will not be considered here.

The aging behavior of glassy polymers--variously referred to as nonequilibrium behavior, enthalpy or volume recovery (relaxation), or simply physical aging--results from the inherent kinetic nature of the glass transition. As a polymer is cooled in a normal process from the melt through the glass transition into the glassy state, there occurs a rapid decrease in molecular mobility which parallels a sudden increase in viscosity and modulus as the transition temperature is approached. The polymer molecules are not, in fact, able to reach their equilibrium conformation and packing with respect to temperature, and as the temperature is further decreased the molecules are essentially "frozen" into a nonequilibrium state of higher energy and volume relative to the corresponding equilibrium state at that same temperature. Since the polymer molecules are in a nonequilibrium state, there exists a thermodynamic potential or driving force for them to approach equilibria by undergoing further packing and/or conformational rearrangement. Although the molecular mobility is greatly decreased in the glass as compared to the rubbery region, it remains finite thus allowing the molecules to approach the equilibrium state corresponding to normal liquidlike packing. Two of the measurable thermodynamic state functions, enthalpy and volume, have been found to decrease with sub-T_g annealing time (at a fixed temperature) as the excess enthalpy and volume originally quenched into the system decrease. Associated with these changes are changes in the physical and mechanical properties of the polymer system [1]: an increase in density, tensile and flexural yield stress, and elastic modulus; a decrease in impact strength, fracture energy, ultimate elongation, and creep rate; and a transition from ductile behavior to brittle fracture.

The utilization of polymers as engineering materials requires that the nature and extent of these changes in properties be fully understood for various types of glassy or partially glassy polymers and necessitates the development of a theory capable of promoting understanding and hopefully allowing prediction of these changes.

A rather extensive body of literature has developed concerning this subject of thermodynamic nonequilibrium in glassy polymers (1, 3). While a complete review is not attempted here, recent trends in experimental and theoretical research are discussed in some depth. In the course of this presentation a clear picture of the basics of nonequilibrium behavior hopefully will be developed for the benefit of those not already familiar with the area, with an emphasis placed upon changes in material properties.

II. THE NATURE OF THE GLASS TRANSITION AND THE GLASSY STATE

Before delving into the thermodynamic and kinetic aspects of nonequilibrium behavior, it will be useful to briefly consider the glass transition itself. An understanding of the origin and nature of the glass transition, both qualitative and quantitative, is necessary to acquire a reasonable understanding of nonequilibrium behavior. Theories which have been developed to describe the glass transition or transition region are indeed the starting points for present theories of the nonequilibrium behavior of polymer glasses. Thus, a brief overview of the glass transition theories presented here will be useful in later discussions when the theories of nonequilibrium behavior are considered.

A. Free Volume Theory

The glass transition temperature is often defined as the temperature at which the thermal expansion coefficient changes in going from the rubbery to the glassy state [4,5]. As shown in Figure 1, a specific volume-temperature plot obtained from dilatometric measurements on poly (vinyl acetate) shows a change in slope at the glass transition. However, as is well known, the glass transition temperature may indeed vary depending upon the rate of cooling or heating. These aspects will be discussed in detail later with respect to nonequilibrium behavior.

The concept of free volume first found utility in describing the transport properties of viscosity and diffusivity in liquids [6]. These properties are considered to be a function of the free volume, V_f, defined by

$$V_f = V - V_o(T) \tag{1}$$

where V is the total macroscopic volume and V_o is the volume occupied by the molecules. This occupied volume includes both the volume within the Van der Waals radii and that volume associated with molecular vibrations. The fractional free volume, $f = V_f/V$, may then be expressed as

$$f = f_g + \alpha_f(T - T_g) \tag{2}$$

where f_g is the fractional free volume at the glass transition, T_g, and α_f is the coefficient of expansion of the free volume. The value of α_f is often considered to be constant over the temperature range of interest.

In its simplest form, the free volume theory defines the total macroscopic volume as

$$V = V_o[1 + \exp\{(\epsilon_h + p\gamma_h)/RT\}] \tag{3}$$

where ϵ_h and γ_h are the energy and volume of holes, respectively, and p is the pressure [7]. Methods are available for determining the various parameters in this expression. It might be noted here that this type of equation is not often very accurate for glassy polymers due to their inherent nonequilibrium nature.

Although the WLF (Williams-Landel-Ferry) equation (5,8,9) was originally deduced empirically to describe time-temperature superposition behavior with respect to mechanical properties, it has also had an important part in the development of the free volume theory, and, in fact, will be used in some of our subsequent discussions of nonequilibrium theories. The basic WLF equation may be written

$$\log a_T = \frac{C_1(T - T_s)}{C_2 + (T - T_s)} \tag{4}$$

where the so-called shift factor $a_T = \eta_T/\eta_{T_s}$ (η represents viscosity) or τ_T/τ_{T_s} (τ represents a characteristic molecular or segmental relaxation or retardation time) and T_s is a reference temperature. When this reference temperature is T_g, the values of the constants C_1 and C_2 become nearly universal for amorphous polymers. A semiquantative theoretical treatment was put forth that could account for the WLF equation--it began with the Doolittle viscosity equation [10] which is

$$\eta = a \exp\left(\frac{b}{f}\right) \tag{5}$$

where a and b are constants. Using the definition of a_T and Eq. (5) gives the relationship

$$\ell n\ a_T = b\ (\frac{1}{f} - \frac{1}{f_g}) \tag{6}$$

Substituting Eq. 2 into Eq. (6) gives

$$\log a_T = - \frac{(b/2.303\ f_g)(T - T_g)}{(f_g/\alpha_f) + T - T_g} \tag{7}$$

which is of the form of the WLF equation. Thus it was shown that the WLF equation, which was originally deduced empirically, could be derived on the basis of free volume theory [4].

The WLF equation with T_g as the reference temperature, as described above, may be written

$$\log a_T = \frac{C_1(T - T_g)}{C_2 + (T - T_g)} \tag{8}$$

The nearly universal constants normally employed are $C_1 = -17.44$ and $C_2 = 51.6$. Since $a_T = \eta_T/\eta_{T_g}$, the WLF equation suggests that at $T = T_g - 51.6$ the viscosity of the polymer material becomes infinite. One of the explanations for this anomaly was proposed by Cohen and Turnbull [11,12]. Their approach was essentially to modify the free volume theory so that changes in free volume with temperature relate to a discontinuity at a temperature T_β below T_g instead of at T_g. T_β is the first secondary transition below T_g. They suggested that the free volume, V_f, corresponds to that part of the excess volume, $V - V_o$, which can be redistributed without a change in energy. (The fractional free volume, $f = V_f/V$, is gererally considered to be 0.025 for most polymers at their respective glass transition temperature.) In other words, only voids or "holes" which are larger

than a certain critical volume constitute the free volume contributing to mobility. Using this formulization, Cohen and Turnbull [12] showed that the viscosity can then be expressed as

$$\eta = a \exp\left(\frac{B'}{T - T_\beta}\right) \tag{9}$$

where a and B' are constants and

$$\tau = \tau_o \exp\left(\frac{B'}{T - T_\beta}\right) \tag{10}$$

When $T_\beta = T_g - 51.6$, the WLF equation is again obtained.

Use of "free volume" arguments will be utilized within the more detailed papers which follow; in particular, the reader is referred to the work of Matsuoka.

B. Thermodynamic Theory

The prediction by the WLF equation that viscosity becomes infinite at $T = T_g - 51.6$ has also been approached from the thermodynamic viewpoint by Gibbs and DiMarzio [13,14] and Adam and Gibbs [15]. Gibbs and DiMarzio proposed that the dilatometric T_g discussed earlier is simply a kinetic manifestation of a true equilibrium second-order transition. A second-order transition is one in which the second partial derivative of the Gibbs free energy is discontinuous at the transition point. Ehrenfest [16] derived thermodynamic equations based upon this definition which clearly show that a second-order transition occurs only when equilibrium exists on both sides of

the transition [17]. Adam and Gibbs have derived the WLF equation using the assumption of Gibbs and DiMarzio as a basis. Assuming that the frequency of molecular jumps is expressed by

$$\nu_c = A \exp\left(-\frac{n\Delta G^*}{kT}\right) \tag{11}$$

where A is a constant, ΔG^* is the barrier height for internal rotation per segment, and n is the number of segments acting cooperatively to make a conformational rearrangement. The conformational entropy per mole of segments is

$$S = \left(\frac{N_A}{n}\right)s_n \tag{12}$$

where N_A is Avogadro's number and s_n is the entropy of a unit of n segments. The frequency of molecular jumps is then given by

$$\nu_c = A \exp\left(\frac{-N_A\, s_n \Delta G^*}{SkT}\right) \tag{13}$$

The conformational entropy of the system, S, is assumed to be zero at the thermodynamic transition temperature T and thus n becomes infinite. The conformational entropy may thus be calculated by

$$S(T) = \Delta C_p \ln\left(\frac{T}{T_\beta}\right) \tag{14}$$

where ΔC_p is the difference in specific heat between the supercooled liquid and the glass at T_g and is assumed constant. Substituting this into Eq. (13) leads to

$$\nu_c = A \exp\left(\frac{-N_A \Delta G^*\, s_n}{k\Delta C_p (T - T_\beta)}\right) \tag{15}$$

This gives a relaxation time of the form of Eq. (10) which was previously shown to be equivalent to the WLF equation.

Thus the WLF equation can also be derived using thermodynamic arguments. The assumption that T_g is a true second-order thermodynamic transition is the basis for this derivation of the WLF equation. A more thorough discussion of this assumption, as well as many other aspects of the thermodynamics of the glassy state, is given by Rehage and Borchard [17].

III. THE NONEQUILIBRIUM BEHAVIOR OF GLASSY POLYMERS AND ITS EFFECT UPON MATERIAL PROPERTIES

The complex behavior of polymeric materials near and below the glass transition temperature has been an area of intensive research for many years. The basic principles of nonequilibrium behavior are introduced here, utilizing results of some of the more recent experimental work as they relate to nonequilibrium behavior. Following this introduction, attention will be focused upon how nonequilibrium behavior influences the properties of various types of polymer systems.

A. The Origin of Nonequilibrium Behavior

It was stated earlier that the nonequilibrium behavior of glassy polymers results from the inherent kinetic nature of the glass transition. Thus, as a polymer is cooled at a finite rate through T_g, the molecular mobility decreases to the point where the molecules are not able to reach their equilibrium conformation in the time frame of cooling. The glass transition would occur at a lower temperature for a slower cooling rate, since the slower cooling rate would allow the

molecules more time to approach their equilibrium state.[+] The important relationship between the time scale of an experiment and the time required for molecular motion is well known for mechanical property testing of polymers. This relationship is appropriately described by the Deborah number, N_{De}, such that

$$N_{De} = \frac{\lambda_c}{t_s} \tag{16}$$

where λ_c is a characteristic time for a material, defined as the time required for the material to reach 1/e of its ultimate elastic response to a step change, and t_s is the time scale of the experiment [18]. Thus an elastic response will result in a high Deborah number, whereas a viscous response will be reflected by a low Deborah number. For example, in a stress-strain experiment carried out at a high strain rate, a polymer may display brittle behavior (small t_s, high N_{De}), while if strained slowly the same polymer may show ductile behavior (large t_s, low N_{De}). At the high strain rate the molecules are not mobile enough to respond at the

[+]The authors wish to point out a somewhat simple minded analogy with the formation of a nonequilibrium structure upon cooling. Specifically, consider an amorphous linear macromolecular system somewhat as a mass of moving well-entangled long earthworms. As these worms are "cooled" their lower mobility (equivalent to loss of kT or thermal energy) makes it less likely that the worms will be able to rearrange themselves to a new equilibrium structure. As the cooling occurs a temperature is reached where within the time scale of observation, further significant backbone motion (cooperative motion of the worm) does not occur. One notes the statement above considers the variable of time.

rate required by the experiment, and the stress is relieved by fracture. When strained slowly the molecules are able to respond within the time scale of the experiment by rearranging to reduce the stress. Thus we have the interplay between a molecular response or relaxation time and the time of the experiment. This same concept applies to polymers as they are cooled from above T_g. At slower cooling rates molecular relaxations and/or rearrangements having relaxation times on the order of the time scale of the experiment will occur, while at higher cooling rates these same relaxations will not be observed.

Since some relaxations may require reasonably long times at lower temperatures, at any finite cooling rate the polymer molecules are thereby likely quenched into a state of higher energy and volume relative to their equilibrium values. Due to a thermodynamic potential for the molecules to approach the state of lowest energy, they may slowly undergo rearrangement in the glassy state in an effort to reach equilibrium. The rate of approach toward equilibrium is governed by the mobility, M, of the molecules as shown in Figure 2. This graph shows that the mobility decreases with an increasing degree of packing in a way that one might deduce intuitively.

The conformational changes which occur in amorphous PET during this approach to equilibrium have been followed by Ito et al. [19]. These investigators monitored the change in intensity of the absorption band at 973 cm^{-1}, which is due to the trans conformation-$\overset{H}{\underset{H}{C}}$-O-vibration, and found that it decreases with annealing time below T_g. Thus the approach to equilibrium in PET involves conformational rearrangements of the polymer molecules with the relative amount of gauche conformation

increasing. Moore and O'Loane (see this issue), utilizing Fourier transform infrared spectroscopy, have also observed an increase in the amount of gauche conformations upon annealing amorphous PET below the glass transition [20].

It was mentioned earlier that changes in free volume may occur by a redistribution of holes [11,12]. The rate of this process is determined by the segmental mobility, M, giving the following closed-loop scheme: V_f determines M which determines the rate, dV_f/dt, of change of V_f, which in turn determines V_f. This may be represented symbolically as follows [3,21,22].

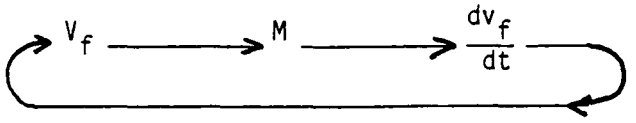

(17)

This scheme suggests that volume relaxation, the change of volume on annealing, is a non-linear phenomenon.

It is then realized that the basic property that changes upon annealing below T_g is the segmental mobility, M. The mobility is directly related to the relaxation times of the polymer, and thus aging may be studied by using tests which relate to the relaxation spectrum. Primarily creep [3] and stress relaxation [23,24] experiments have been used in this regard. The small strain creep curves of poly(vinyl chloride) (PVC) are shown in Figure 3 as a function of annealing time below T_g. It can be seen that the curves are shifted to the right by one decade for each tenfold increase in sub-T_g aging time when sub-T_g annealing temperature is held constant. This suggests that under these conditions aging is linear with respect to logarithmic time. Using

another mechanical parameter, Figure 4 shows stress relaxation data determined at one percent strain on a crosslinked epoxy system, and presented as the percent relaxation in stress that occurs in ten minutes *vs* logarithmic sub-T_g annealing time. This plot also suggests that aging is correlated to the logarithm of the sub-T_g storage time. These data show unequivocally that aging affects creep and stress relaxation by primarily changing the retardation and relaxation times, respectively.

The curve in Figure 4 reached an *apparent* equilibrium value of percent stress relaxation after about 2000 minutes of sub-T_g annealing. From the data, one might be tempted to say that an actual equilibrium state has been reached at this point, but this has proven not to be the case. Matsuoka, *et al.* [23] obtained stress relaxation data for polystyrene aged below T_g for different times, as is shown in Figure 5. These curves show very little variation between the samples with different aging histories during the first part of the stress relaxation experiment. However, as the stress relaxation experiment proceeds, the relative behavior of the different samples varies greatly. The first part of the curves--that part which shows the decrease in stress during the first few minutes after the stress relaxation experiment is begun--is seen to approach a single curve with sub-T_g annealing time, and for samples aged for longer times the curves actually coincide. Thus, it is expected that an "equilibrium" value of percent stress relaxation during the first few minutes of relaxation would be observed for these polystyrene samples annealed for longer periods of time. Data to further support this explanation will be presented later in this paper.

One point that might have been noticed in the creep curves of Figure 3 is that all of these curves can be superimposed by an almost horizontal shift to form a master curve. This has also been found true for stress relaxation curves. Both Struik [3] and Matsuoka *et al.* [23] have confirmed this shifting behavior for many polymers, including polystyrene [3,23], poly(vinyl chloride) [3,23], polycarbonate [3,23], poly(ethylene terephthalate) [3], polypropylene [3], etc., and even for nonpolymeric materials which show glass transition behavior, such as bitumen, shellac, and amorphous sugar [3]. These data support the earlier statements that aging primarily affects the retardation and/or relaxation times, and that aging results from the inherent kinetic nature of the glass transition. The shifts between successive creep (or stress relaxation) curves are approximately constant, and are defined by log "a", where the parameter "a" is taken as positive for a shift to the left. The *aging rate* may therefore be defined as

$$\mu = \frac{-d \log \text{"a"}}{d \log t_e} \tag{18}$$

where μ is the shift rate, "a" is the acceleration factor, and t_e is the aging time [3].

The plot of -log "a" *vs* log t_e shown in Figure 6 shows that the shift rate is approximately constant between t_e = 0.3 day and t_e = 1000 days, giving a shift rate of about unity. Figure 7 shows a plot of shift rate *vs* temperature for several different polymer systems. As expected, for all of the polymers μ is zero above T_g. There is a rapid increase in μ below T_g to about unity and then a decrease which occurs at different

temperatures for the various systems. The reason for this behavior will now be discussed here.

Struik [3] has suggested that at a given sub-T_g temperature the segmental mobility, M, is inversely proportional to the aging time,

$$M \sim \frac{K_1}{t_e} \tag{19}$$

Since the relaxation times are also inversely proportional to M, he suggests they should increase proportionally with the aging time. This explains why the shift rate, μ, is nearly constant throughout the thermal aging range and why it is approximately unity. Struik's derivation of equation (19) is not valid near equilibrium, and thus the decrease of μ near T_g is expected.

The decrease in M at low temperatures is explainable by the free volume theory. At the highest secondary transition, T_β, segmental mobility decreases greatly due to a lack of sufficient free volume. Secondary relaxations may still persist below T_β, but they do not cause the polymer to physically age since they apparently do not result in a change of free volume and thus relaxation behavior [3]. Referring again to Figure 7, it is seen that the aging range of these polymers occurs between T_β and T_g. That polymers only age in a certain temperature range has thus been determined experimentally and explained by the free volume theory [3].

During the quenching process from the melt to the glassy state, as well as during the cure of thermosets, temperature gradients develop within the polymer materials due to their rather low thermal conductivity.

These temperature gradients, in turn, may result in the formation of stress gradients through the material [25,26,27]. While we will not discuss the consequences of thermal stress gradients and their time dependence on the behavior of bulk glasses, an awareness of this quenching or rapid cooling effect must be recognized.

B. Effect Upon Material Properties

1. Amorphous Linear Homopolymers

Most experimental work reported in the literature has been performed on purely glassy linear homopolymers. The study of these systems has not only provided a general understanding of how nonequilibrium behavior influences the properties of a polymer material, but it has also indicated the need to be aware of physical aging processes in engineering applications involving glassy polymers. The effects of nonequilibrium behavior, or physical aging, upon the properties of a glassy polymer can be quite dramatic. Let us now present a brief overview at how many of the various properties of a glassy polymer may be affected by the physical aging process.

Volumetric Properties

It has already been emphasized that after a polymeric material is quenched from above to below the glass transition temperature, there is a decrease in free volume as the molecules approach the state of normal liquidlike packing by undergoing conformational rearrangements. Thus any quenched in excess specific volume will decrease as the system approaches its equilibrium value upon annealing below the glass transition temperature provided that backbone motion is possible.

Interestingly, Goldbach and Rehage [28] have shown that the same equilibrium value is approached by polystyrene from both excess and deficient volume states, as is shown in Figure 8. The inherent asymmetry and non-linearity observed in the expansion and contraction curves will be discussed in more detail later.

External pressure has also been found to influence glass formation in polymers. Figure 9 shows the pressure dependence of the volume-temperature plots of polyvinyl acetate as determined by McKinney and Goldstein [29]. It is clear that the glass transition temperature (temperature at which the slope changes) increases significantly with increasing external pressure, a direct result of the decrease in molecular mobility as pressure and density are increased. The magnitude of this increase is generally 15-25°C per 1000 atm [5].

To this point, our discussions have only involved nonequilibrium behavior at a single temperature. In many cases the thermal history of a sample may be more complicated than a simple quench from above T_g. Suppose that a sample at equilibrium above T_g is quenched to a temperature T_1 below T_g, stored for a time t_1, and then heated to a testing temperature T at which it is tested at some specified time. Results of such volumetric studies on polyvinyl acetate (II) have been reported by Kovacs [30] in a now classic paper, and are shown in Figure 10. The observed volume relaxation peaks are an example of the extremely complex property behavior of glassy polymers. The origin of these "memory effects" will be made clear during our later discussion of the free volume theory as applied to nonequilibrium behavior.

Thermal Properties

Changes that occur in the thermal properties of glassy polymers during annealing below the glass transition temperature have often been monitored using differential scanning calorimetry (DSC) [1, 31, 32]. (Also see papers within this issue.) For an unannealed glassy material, there is normally a baseline shift in the DSC plot (heat capacity vs temperature) corresponding to the change in the specific heat of the glass, C_g, to that of the liquid state, C_f. A typical baseline shift for a freshly quenched sample is shown in Figure 11b by the lower solid line. The corresponding enthalpy-temperature plot is shown by the solid line in Figure 11a. Referring to Figure 11a, the physical aging process may be described as follows. The sample is cooled at a rate r_1 from above T_g (r_1) to T_A. During sub-T_g annealing for a period of time, t, at T_A, the enthalpy is reduced to H_t by the process of physical aging. (The equilibrium enthalpy at T_A is H_E.) Heating at a similar rate r_1, there is an absorption of energy at T_g (r_1), due to the increased level of segmental mobility, with a step increase in enthalpy being used here for simplicity. Such an approximation is reasonable when the amount of energy absorbed is large, which is generally about a calorie per gram or more [33]. This energy absorption is reflected in the DSC scan as an endothermic peak at T_g, as is shown in Figure 11b.

The amount of energy absorbed in the DSC scan is reflected in the size of the endothermic peak per unit mass of amorphous material. Thus, since the excess enthalpy decreases during annealing, the enthalpy recovered during heating increases with increasing annealing time, and the endothermic peaks become correspondingly larger. This is depicted

in Figure 12, where the DSC scans were performed on amorphous PET annealed for various times at 23°C.

Petrie [31] has followed enthalpy changes for polystyrene annealed at 365 K (T_g = 373°K), and this data, as shown in Figure 13, depicts the approach of the excess enthalpy to its calculated equilibrium value at this temperature. Figure 14 shows these data, plotted as (Q_E - Q_t) *vs* logarithmic sub-T_g annealing time, where Q_E is the amount of energy absorbed when the system is in its equilibrium glassy state and Q_t is the amount of energy absorbed at a particular time following quenching. Once again, a linear dependence is noted. Additional enthalpy recovery data are also shown for annealed polystyrene having various thermal histories.

Frosini, *et al.* [34] have suggested that a linear relationship exists between the thermal energy, Q, absorbed in the transition region and the temperature of the absorption peak, given by

$$Q = (C_{p_\ell} - C_{p_g}) (T_p - T_g^*) \qquad (20)$$

where C_{p_ℓ} is the heat capacity above T_g, C_{p_g} is the heat capacity of the glass, T_p is the temperature of the endothermic peak, and T_g^* is the glass transition temperature of the quenched glass. Figure 15 shows such a relationship for poly (phenylacrylate) annealed at three different temperatures for a variety of annealing times. These workers also performed isothermal enthalpy absorption studies in which annealed glassy polymers were heated to above the point where the enthalpy-temperature plot for the annealed glass intersects the equilibrium liquidus line, but not to the temperature where the enthalpy absorption occurs. At some intermediate temperature heating was stopped and enthalpy was monitored

as a function of time. Results of such experiments on poly(vinylbenzoate) are shown in Figure 16a, where DSC traces for isothermal enthalpy absorption are plotted as a function of time for various temperatures. Figure 16b shows the time-temperature diagram for the isothermal glass-liquid transformation of poly(vinylbenzoate), where t_p is the time of the absorption peak at temperature T. This information may be put in Arrhenius form by plotting ln (t_p) versus 1/T. The value obtained for the activation energy for enthalpy recovery is 263 kJ/mole, in good agreement with prior results using different heating rates [34].

Brown, et al. [36] have also reported DSC and dilatometric studies on densified polymeric glasses. Their work showed that the volumetric behavior of densified glasses is that which would be expected; i.e. glasses formed under increased pressure show a decrease in specific volume with increasing pressure. However, enthalpy decreases initially with increases in glass formation pressure, while glasses formed under much higher pressure have enthalpies above the enthalpy of the glass at atmospheric pressure. This behavior is illustrated schematically in Figure 17, and shows that the glass transition temperature, as defined by enthalpy [$T_g(H)$] or volume [$T_g(V)$] behavior, vary significantly for polymeric glasses formed under high pressures. Indeed, $T_g(H)$ and $T_g(V)$ appear to diverge with increasing densification pressure. This behavior has yet to be explained satisfactorily. It is but another example of the complex behavior displayed by polymeric materials within the glass transition region.

Mechanical Properties

Changes that occur in the mechanical properties of glassy polymers upon sub-T_g annealing have already been considered to some extent earlier in this paper. In particular, the effects upon creep and stress relaxation behavior have been indicated.

In general, it may be said that a glassy polymer becomes more brittle with the aging process. As the free volume decreases molecular response to imposed stress becomes progressively slower, resulting in an embrittlement phenomena. This has been clearly demonstrated by Mininni, et al. [37] for amorphous poly(ethylene terephthalate) (PET). Figure 18 shows tensile stress-strain curves obtained at 22°C for PET annealed at 51°C for the times indicated. It is clear that annealing results in a transition from ductile to brittle behavior, causing a dramatic increase in yield stress and a decrease in yield strain. This behavior has also been observed in other linear glassy polymers, such as polycarbonate (PC) [38-41]. Although Young's modulus is not as sensitive to the molecular changes arising during annealing, it has been shown to increase as well for PET, PC, and some linear epoxies [42]. The increase in Young's modulus is again due to the shifting of the retardation spectrum to longer times, i.e., as free volume and molecular mobility decrease when the material is aged, retardation mechanisms (molecular response) become progressively longer due to the increased time required for molecular rearrangements to occur. Thus, when samples annealed below T_g for a short time are stretched, their high molecular mobility, as contrasted with longer time annealed samples, allow more rapid rearrangement of the polymer molecules in reducing stress, and thus stress increases at a

slower rate. When samples annealed below T_g for longer times are stretched at the same rate, reduction in stress by molecular rearrangement is slower, and thus stress increases at a faster rate. Similarly, the increase in yield stress with sub-T_g annealing occurs because, as molecular mobility is decreased upon annealing, a greater amount of energy is necessary to initiate the molecular motions associated with yielding.

Dynamic Mechanical Properties

The effect of physical aging upon the dynamic mechanical properties of linear glassy polymers has been best illustrated by Petrie [1, 32] and by Wyzgoski [56]. Studies by the former worker on polystyrene have demonstrated that changes in the dynamic mechanical properties upon sub-T_g annealing correlate to changes in the excess enthalpy for the same aging conditions [32].

Figure 19 shows plots of the shear storage modulus, $G_1^{\cdot}$, the logarithmic decrement, Δ, and the enthalpy recovery, ΔH, for quenched atactic PS vs annealing time at 92°C. The general correspondence between the dynamic mechanical properties and enthalpy is clear.

Further experiments by Petrie were performed to investigate the relationship between the dynamic mechanical and enthalpic properties of PS [32]. PS which had reached equilibrium at 92°C and was then heated to 95°C showed a decrease in shear storage modulus and an increase in logarithmic decrement, behavior which was the opposite of that observed for a direct quench to the same temperature. As might be expected, however, the values that the shear storage modulus, logarithmic decrement,

and enthalpy recovery approached in this case were the same as those approached after a quench directly to 95°C, thus suggesting that the same final state is attained whether it was approached from a state having "excess" or "deficient" thermodynamic properties [32].

Flick and Petrie have recently reported results of a similar study to correlate changes in both mechanical and dynamic mechanical properties with changes in the excess enthalpy for bisphenol-A polycarbonate [43]. Previous studies had been inconclusive, since the morphology and physical properties of thin films which had been annealed below T_g could not be fully restored without heating the films above the melting point [44]. Flick and Petrie, who were able to correlate changes in the mechanical, dynamic mechanical, and enthalpic properties of this material, conducted their annealing in dry nitrogen. They suggest that the discrepancies in earlier work may have been due to inadequate conditioning of the sample prior to and during sub-T_g annealing. Specifically, bisphenol-A polycarbonate films annealed without protection from the atmosphere may degrade substantially, hence T_g can be lowered, and prespherulitic structures developed caused by crystallization of the degradation (hydrolysis) products.

Dielectric Properties

Uchidoi, et al. [45] have studied volume, enthalpy, and dielectric polarization relaxation for PS and poly(vinyl acetate)(PVAC). Figure 20a shows the frequency dependence of dielectric loss factors of PVAC, calculated by Fourier transformation of the transient currents obtained at various times following a quench from 55°C to 31°C (T_g = 43°C).

Figure 20b shows the annealing time dependence of the frequency where dielectric loss is a maximum. Clearly, this frequency decreases linearly with logarithmic annealing time until an apparent equilibrium value is reached. The time scale of this relaxation process was observed to be about the same as that for volume relaxation. Johnson, et al. [46] have reported results of a similar study on PVAC, in which sub-T_g annealing was conducted at 19°C. They found that for recovery at this temperature, there was excellent agreement between the enthalpic and dielectric data.

Diffusion Properties

Chan and Paul [47,48] investigated the sorption of CO_2 in polycarbonate (PC) having different thermal history. As shown in Figure 21, the amount of CO_2 sorbed at 35°C is dependent upon the annealing time at 125°C (T_g = 150°C). Annealing the polymer at 125°C results in a reduction of free volume and therefore a reduction in the available space for sorption of CO_2. As can be seen from the figure, the amount of CO_2 sorbed at each pressure decreases with increased annealing time at 125°C, clearly a result of the decreased free volume.

Ophir [49] and Kong, et al. [50] have reported that solvent uptake in network epoxy systems often proceeds in a non-Fickian, relationship with time. The kinetics of solvent uptake were indeed found to be related to sub-T_g annealing time, presumably due to the decrease in free volume with annealing time.

A practical aspect of the dependence of solvent absorption kinetics upon thermal history of the polymer has been observed by Petrie [51].

She has found that the dyeability of certain synthetic fabrics depends upon the age of the fabric, an effect which is almost certain to be due to loss of free volume with sub-T_g annealing.

2. More Complex Polymer Systems

As can be seen from our discussions concerning nonequilibrium behavior of glassy polymers, almost all experimental work reported in the literature has been performed on purely glassy linear homopolymers. However, this class of polymers constitutes only a small portion of all of the polymers presently used in applications. We will now briefly focus on some rather recent investigations of nonequilibrium behavior in such complex systems as polymeric network glasses, semicrystalline polymers, and block and graft copolymers.

Polymeric Network Glasses

Although it has been previously shown that network epoxies undergo physical aging [3], it was only relatively recently that more complete studies on epoxy network systems and rubber-modified derivatives were completed [24,50,52]. Ophir, et al. [24] performed stress-strain, stress relaxation, and differential scanning calorimetry studies on a series of unmodified and rubber-modified epoxies. Figs. 22a&b illustrate one example of the stress-strain behavior of these systems. In general, it is clear that both the rubber-modified and unmodified epoxy systems experience an embrittlement phenomena due to physical aging. It should be made clear that the observed time dependent changes in these crosslinked glasses do not arise from further curing. This can be demonstrated for example by reheating the samples in Fig. 22_A above T_g and requenching to below T_g

as before. Again, one will note that initially the freshly quenched material will be more compliant and will embrittle with time as before. That is, the time dependent changes are reversible. In some network glasses, however, that are not completely cured, then,depending on the storage (sub-T_g) temperature, further crosslinking may slowly take place at a rate limited by diffusion of a reacting species. These time dependent changes often vary with log time as well but, of course, these are not reversible and thus may be separated in principle from the physical aging process. As given earlier in Fig. 4, the ten minute stress relaxation data for the unmodified epoxy, was plotted versus logarithmic sub-T_g annealing time. As discussed before, the decrease in percent stress relaxation is due to the decrease in segmental mobility of the network chains arising from the physical aging process. The two-phase rubber-modified epoxies show similar behavior. The enthalpy recovery characteristics as determined via DSC techniques for the unmodified epoxy are shown in Figure 23 as a function of annealing temperature at constant sub-T_g annealing time. The magnitude of the enthalpy recovery from the quenched state (area under the "aging peak") was again found to be related linearly to logarithmic sub-T_g annealing time.

Semicrystalline Polymers

Physical aging of the glassy regions in semicrystalline polymers has been shown to affect the bulk properties of these materials by Struik [3] and Tant and Wilkes [53,54]. The latter authors studied the characteristics of the physical aging process in semicrystalline poly(ethylene terephthalate)(PET) as a function of crystalline content. Figs. 24a&b show

plots of percent stress relaxation at about one percent strain for ten minutes of relaxation versus sub-T_g annealing time at 23°C for an amorphous PET sample and another of 29 percent crystalline content. In both cases it is seen that an "apparent" equilibrium value of percent stress relaxation for this experiment is reached just past 1000 minutes. As discussed earlier in this paper, this apparent equilibrium does not indicate that an actual equilibrium state has been reached and that physical aging has stopped. It has been demonstrated that had a longer time "window" than 10 minutes been used to determine the percent stress relaxation, the apparent equilibrium would have been reached at a longer annealing time [54]. Carrying out these studies on additional samples, the stress relaxation rates (in 10 min.) were determined as a function of crystallinity content and sub-T_g annealing time. It was found that sub-T_g annealing time dependence decreased with increasing crystallinity. In fact, the dependence extrapolated to zero for a one hundred percent crystalline polymer [42,54].This behavior, of course, is expected on the basis that as crystallinity increases, the fraction of amorphous glassy material decreases and likewise does the amount of material that will display physical aging. That is, for a one hundred percent crystalline system, no physical aging would occur.

Finally, to demonstrate the overall effect of physical aging on stress strain behavior of semicrystalline PET, Figs. 25a&b are presented. It is clear for these data that the parameters of Young's modulus, yield stress and yield strain are very time dependent with respect to sub-T_g annealing.

Systematic investigation of such variables as crystal orientation and variation in morphological texture (but with equal crystallinities) has

not yet been studied by researchers. In view of the wide usage of crystalline polymers that possess a glassy fraction at the use temperature, such future studies would certainly be warranted.

Block and Graft Polymers

Tant and Wilkes [55] have recently observed that physical aging of the glassy component in styrene-butadiene (SBS) and polycarbonate-siloxane block copolymers affects the bulk properties of these polymers. Furthermore, the extent of these property changes is expected, i.e. it increases as the fraction of glassy polymer present increases. Likely, the magnitude of the physical aging effects in these and related two-phase systems having a glassy component would be dependent upon the morphological continuity of this same component. Again, systematic studies in this vain are presently lacking.

Wyzgoski [56] and Booij and Minkhours [57] have carried out interesting physical aging studies upon ABS systems and have clearly demonstrated that the effects are very significant with regard to the sub-T_g time dependent thermal and mechanical property behavior. The latter study in particular proposes a scheme for predicting the mechanical property behavior once given the exact thermal history of the material.

IV. THE THEORIES OF NONEQUILIBRIUM BEHAVIOR

To this point our discussions have only provided a qualitative and pseudomolecular description of the nonequilibrium condition of glassy polymers, and how this condition, in turn, affects the material properties of polymer systems containing glassy regions. We now turn our attention to an overview of some of the many theories which attempt to describe

nonequilibrium behavior in a quantitative manner. Much of this work is still in development. Indeed, this volume also contains papers by Aklonis and Matsuoka that focus extensively on these theoretical approaches.

A. Thermodynamic Approaches

Most of the early attempts to quantitatively describe the glass transition and the glassy state in polymers utilized thermodynamic principles [13-15,58-60]. We have already discussed some aspects of this thermodynamic development, in particular the derivation of the WLF equation from thermodynamics. In keeping with the title of this paper, i.e., a discussion of recent trends in the development of the theory of nonequilibrium behavior, we will not attempt to thoroughly discuss these thermodynamic approaches. Suffice it to say that these efforts have had some successes and failures, but purely thermodynamic treatments have been as yet unsuccessful in quantitatively describing the complex behavior of polymers within the glass transition region. Nevertheless, these thermodynamic approaches are an important consideration in gaining a complete understanding of the glassy state. The interested reader should consult a recent review by Rehage and Borchard [17].

B. Phenomenological Approaches

The phenomenological theories that have been developed to date attempt to model the complex time dependence of the properties of polymers in the glass transition region. In general, these approaches fall into two different categories: single parameter models or multi-parameter models. The first approach we will consider belongs to the

former category. Although it is probably the simplest model, it is quite useful in qualitatively describing many of the characteristics of the nonequilibrium behavior of glassy polymers.

1. A Single Parameter Model - The Free Volume Theory

In general, the properties of a pure substance in its equilibrium state can be completely determined by specifying temperature and pressure. However, polymers in the glassy state are generally not in thermodynamic equilibrium, and additional ordering parameters are required to specify the state of the system. The free volume theory utilizes a single ordering parameter (i.e. free volume), in addition to temperature and pressure, in an attempt to describe the nonequilibrium glassy state. The various single parameter models, including the free volume theory, have been reviewed in detail by Kovacs [30], therefore only an introduction to this treatment will be given here.

For isobaric volume recovery, Kovacs [30] proposed the equation

$$\frac{dV}{dt} = \alpha_g V_\infty q - \frac{V - V_\infty}{\tau} \qquad (21)$$

where $q = dT/dt$ and is the rate of cooling or heating, V and V_∞ are the actual and equilibrium specific volumes respectively, $\alpha_g = V_\infty^{-1}(\partial V/\partial T)_P$ is the thermal expansion coefficient of the glass, and τ is the volume retardation time at constant pressure P. Defining $\delta = (V-V_\infty)/V_\infty$, equation (21) may be rewritten as

$$-\frac{d\delta}{dt} = \Delta\alpha \cdot q + \frac{\delta}{\tau} \qquad (22)$$

Enthalpy recovery may be described by replacing δ in equation (22) by $\delta_H = (H-H_\infty)/H_\infty$ and $\Delta\alpha$ by ΔC_p. The quantities $\Delta\alpha$ and ΔC_p are the differences in α and C_p between the supercooled liquid and the glass at T_g. Utilizing the Doolittle viscosity equation (equation (5)) and following reasoning similar to that used in deriving equation (6), leads to

$$\tau = \tau_g \exp\left(\frac{b}{f} - \frac{b}{f_g}\right) \tag{23}$$

where τ is the volume retardation time, τ_g is the volume retardation time in equilibrium at a reference temperature T_g, f is the fractional free volume, and f_g is the fractional free volume in equilibrium at T_g. Substituting equation (23) into equation (22) gives

$$-\frac{d\delta}{dt} = \Delta\alpha \cdot q + \frac{\delta \exp(b/f_g)}{\tau_g \exp(b/f)} \tag{24}$$

Hutchinson and Kovacs [61] derive a similar equation for enthalpy recovery which involves conformational entropy instead of free volume.

We have already discussed some aspects of the free volume theory as it relates to the glass transition and to nonequilibrium behavior. Although it is likely that any single parameter model will have certain limitations in describing the thermodynamic state of a glassy polymer, free volume theory has proven itself extremely useful in qualitatively, and in many cases quantitatively, describing the nonequilibrium behavior observed in glassy polymers. The free volume theory will be discussed here in light of recent advances in the area of nonequilibrium behavior.

Mechanical deformation processes have been observed to have an effect on aging behavior of polymers, and this finding has been explained both by Struik [3] and Matsuoka et al. [23,62] using the free volume theory as

outlined above. It has been observed that tensile deformations, uniaxial compressions and shear deformations totally or partially erase the previous aging of polymers. This may be thought to contradict the free volume theory, since ideal uniaxial compressions and shear deformations theoretically do not increase free volume. However, Struik [3] has suggested that mechanical deformations connected with segmental motion generate free volume, irrespective of whether they are tensile deformations, uniaxial compressions, or shear deformations. Thus, the type of stress field involved is irrelevant to whether or not free volume associated with segmental mobility is created. In fact, Matsuoka and Bair [62] performed an experiment involving pure shear of polycarbonate (PC) and found that there was an enthalpy increase with shear deformation. According to their model, this suggested an increase in free volume with shear. In addition, Matsuoka et al. [23] have proposed a model relating the free volume fraction, f, the tensile strain, ε, and Poisson's ratio, μ, as follows

$$f = f_o + \varepsilon(1 - 2\mu) \tag{25}$$

and have found that the magnitude of the shift with strain, calculated from the WLF equation and equation (25) agrees with experimental data. Struik [3] has suggested that the rate, $\dot{V}_{f_d}$, at which free volume is generated is proportional to the rate of dissipation of mechanical energy, $\dot{W}_{f_d}$:

$$\dot{V}_{f_d} = k\,\dot{W}_{f_d} \tag{26}$$

where k is a constant and the dots denote differentiation with respect to time. Kovacs [30] had previously proposed a theory of volume relaxation:

$$\frac{dV_f}{dt_e} = \frac{-(V_f - V_{f_\infty})}{\tau(V_f,T)} \tag{27}$$

where V_f is the momentary free volume, V_{f_∞} is the equilibrium free volume at temperature T, and $\tau(V_f,T)$ is the momentary value of the relaxation time which is dependent upon both V_f and T. Adding the production rate of free volume due to deformation to the right-hand side of equation (26), we obtain

$$\frac{dV_f}{dt_e} = - \frac{V_f - V_{f_\infty}}{\tau(V_f,T)} + \dot{V}_{f_d} \tag{28}$$

The effect of mechanical deformations upon the free volume is depicted in Figure 26 Assuming that $\dot{W}_d$ is a Dirac pulse at time $t_e = t_{e_1}$ with an intensity ΔW_d, it is seen that the deformation reactivates the volume relaxation process with the relaxation after t_{e_1} being much faster. The free volume theory predicts that with an increase in free volume the previous aging is partially or totally erased. This phenomenon is shown in Figure 27, where the dotted line shows the creep behavior of polyvinyl chloride at 16 hours. A stress, σ_1, is applied at 17 hours and is removed at 17.5 hours. The creep curve following the high stress pulse is shifted to the left, and the sample shows subsequent re-aging as the creep curves are shifted to the right. Thus the stress pulse causes an apparent decrease in the relaxation times and thus partially erases the previous aging, as predicted by the free volume theory. Struik [3] has also found that cold drawing of polyvinyl chloride has the effect of erasing previous aging.

The free volume model may be used to explain the "intermittent loading anomaly" observed when a periodic or intermittent stress is applied [3]. Specifically, the data obtained from a continuous creep test suggests that the free volume is only temporarily disturbed, i.e., it approaches the free volume corresponding to previous aging provided the applied stress is much less than the yield stress. Periodic loading, on the other hand, reduces aging permanently and at long times the aging will be arrested and the segmental mobility will permanently exceed the mobility in either spontaneous aging or continuous creep.

Matsuoka and Bair [62] have found support for the free volume concept by monitoring the temperature of polycarbonate upon deformation. They reasoned that with an increase of free volume upon deformation, there should also be an increase in excess enthalpy and a parallel decrease in temperature. Their results are shown in Figure 28. The temperature follows a path which is almost a mirror image of the stress-strain curve. The temperature reaches a minimum where the polymer begins to yield. At this point there is a temperature rise due to frictional heat generation. Integration of the temperature-strain curve allows estimation of the rate of enthalpy increase per unit strain and taking C_p = 0.26 cal/g, the total enthalpy change is estimated to be 0.2 cal/g for the strain up to 0.05 near the yield point. The same type of behavior was also found for polycarbonate under shear, as was mentioned earlier.

These same researchers also derived the equation

$$H_1 - H_2 = T_g(S_1 - S_2)$$

$$= T_g \phi R(f_1 \ell n f_1 - f_2 \ell n f_2)/M_w \qquad (29)$$

where the subscripts refer to samples at two different annealing times, S is the entropy, M_w is the segmental molecular weight, and f is the fractional free volume. The factor ϕ is the ratio of the total entropy increase to that part of the entropy corresponding to volume increase. Using Kovacs' [30] equation for the relaxation time

$$\tau = k_o^{-1} \exp(1/f) \tag{30}$$

and equation (29), Matsuoka and Bair [62] calculated the excess enthalpy in two ways: first, using simply the area of the endothermic peak, and second, using the more proper procedure, suggested by Richardson and Savill [63], of subtracting area A from area B on the DSC scan as shown in Figure 29. The excess enthalpy values calculated by these two methods, along with the results obtained by Petrie [32], are plotted in Figure 30. It is noted that the free volume theory predicts the observed results quite accurately in this case.

Free volume theory has also been used to predict creep behavior of polymers as a function of annealing time below T_g. Matsuoka et al. [23] have utilized an equation deduced empirically by Kovacs [64], to quite successfully predict the shift in relaxation or retardation times for PVC upon annealing at 60°C. This equation is

$$-\frac{df}{dt} = \frac{f}{\tau} = \frac{f}{\tau_o} \exp\left(\frac{1}{f_o} - \frac{1}{f}\right) \tag{31}$$

where the zero subscript refers to the initial condition. The solution of this equation is the exponential integral,

$$\int \frac{\exp\left[\frac{1}{f} - \frac{1}{f_o}\right]}{f} \, df = \frac{t}{\tau_o} \tag{32}$$

Again, these free volume based equations quite accurately predicted creep curves for PVC which had been aged at 60°C for various times. More detail on using this approach is given by Matsuoka in this same issue.

We have thus seen how the free volume theory has proven to be useful conceptually by describing many of the changes that are observed to occur in glassy polymers. Although most of the success of the free volume theory has been of a qualitative nature, there has been some limited success in utilizing it as a quantitative tool in predicting nonequilibrium behavior. The limitations of the theory, however, prevent its use in all applications.

Struik [3] has shown mathematically that all of the free volume models utilized [8-12,65, 66] have limitations. This, however, should not suggest that the concept of the free volume theory is incorrect. Recall that Turnbull and Cohen [11,12] suggested that the free volume is distributed over holes of various sizes. There would thus be a distribution of holes larger than a critical size which allows mobility. The mobility is therefore not determined by the total free volume, but by the distribution of free volume.

Thus, while the free volume theory is useful in providing a qualitative picture of nonequilibrium behavior, its value as a truly quantitative theory has not been fully realized. In essence, the problems lie in defining the critical free volume unit related to molecular mobility and the distribution of these units within the system in question, and secondly, in being able to measure the actual distribution of free volume.

2. Multiparameter Models

The shortcomings of the free volume theory in quantitatively describing the nonequilibrium phenomenon in polymers have prompted

investigators to search for a theory capable of predicting this behavior. During the last decade several phenomenological models were advanced which utilize a distribution of retardation or relaxation times [2,67-71]. Although the basic assumptions involved with all of the models are similar to those in the original model of Narayanaswamy [67], we will focus on the more recent approach utilized by Kovacs and coworkers [2,69-71]. Additional details on the phenomenological approach can be obtained from the paper by Aklonis in this issue.

Obviously, a satisfactory model must predict the various rather complex types of behavior exhibited by polymers in the glass transition region. Although some of these have been discussed earlier in this paper, it will be worthwhile to briefly review some of the most significant aspects.

Effect of Experimental Rate - As has already been discussed, the glass transition temperature is dependent upon the rate of cooling from the liquid state. At slower cooling rates equilibrium is maintained to lower temperatures before glassy behavior begins, as illustrated in Figure 31a.

Asymmetry - Behavior in the glass transition region is very different for isobaric heating and cooling, as shown by the volumetric changes in Fig. 31b. Cooling isobars resemble a second-order transition, while heating isobars resemble a first-order transition.

Nonlinearity - The nonlinearity of the glass transition is illustrated in Figure 31c, utilizing volume recovery isotherms. Both contraction and expansion isotherms are shown, and both the asymmetry and the nonlinearity of the system response is evident. For symmetric behavior, contraction and expansion isotherms with equivalent positive and

negative initial deviation from volume equilibrium would be mirror images of one another. This is clearly not the case. For linear behavior the response to the larger temperature jump would be three times the response to the smaller temperature jump. Circles are drawn on each isotherm where 10 percent of the recovery has taken place. If the behavior was linear the circles on the contraction isotherms and those on the expansion isotherms would be on straight vertical lines. If the response were both linear and symmetric, all six cirlces would fall on the same vertical line.

Memory - The memory behavior associated with a double temperature jump, briefly discussed earlier, is illustrated in Figure 31d. Again, this behavior occurs when a sample at equilibrium above T_g is quenched to a temperature T_1 below T_g, stored for a time t_1, and then heated to a testing temperature T, still below T_g, at which the sample is tested at a specified time. These volume relaxation peaks have been shown to be the result of a distribution of relaxation or retardation times, this distribution likely being due to the distribution of free volume related to molecular mobility.

Before discussing the specific multiparameter theories, it will be helpful to discuss the origin of the volume relaxation peaks by utilizing a mechanical analogy put forward by Struik [3]. Consider a creep experiment in which a sample in mechanical equilibrium is subjected to a stress, $-\sigma_1$, at time $t = -t_1$. At the time zero the stress is changed to $-(\sigma_1 - \sigma_2)$ where $\sigma_2 < \sigma_1$. The resulting creep behavior is the sum of two creep curves with the strain passing through a maximum. There are two necessary conditions for this maximum to occur: first, there must be a

distribution of retardation times, and second, the time t_1 between the application of the initial stress and the change to a lesser stress should be longer than the shortest retardation times yet shorter than the longest retardation times. If the sample under consideration is represented by the generalized Voigt model, the explanation becomes even more clear. Spring-dashpot units with short retardation times will come to equilibrium soon after application of the initial stress and before the change to a lower stress, but units with longer retardation times will not reach equilibrium during this time period. When the stress is reduced, however, units which have reached equilibrium must return to a new equilibrium condition while those that have not reached equilibrium will simply continue to strain until equilibrium is reached. The strain will then pass through a minimum due to the distribution of retardation times. This model is easily applied to volume relaxation, in which case a distribution in free volume results in a distribution of relaxation times. Considering the quench-storage-upquench scheme, the rapid relaxations will occur soon after the quench from above T_g and during the storage period, but the slower relaxations will not. When the material is heated to a higher temperature, the rapid relaxations will have to return to a new equilibrium condition while the slower relaxations will simply continue in the same direction. After the upquench the rapid relaxations will result in an increase in free volume, while the slower relaxations will continue to decrease free volume. The rapid relaxations will control and the macroscopic observation is an increase in volume. As the rapid relaxations again reach equilibrium, the slower relaxations gain control, a volume peak is passed, and again the volume begins to decrease.

Thus, if one accepts the above model, much of the complex volumetric data can be accounted for on an initial intuitive basis.

The treatment of Kovacs and coworkers [2,69-71] utilizes equation (22) for volume recovery which was originally developed as part of a single parameter model [30]. Clearly, the retardation times should depend not only on temperature and pressure, but also on the actual state of the glass. In fact, one difficult problem for isobaric recovery is the separation of the relative contributions of temperature and structure. In general, the method used is to assign a certain fraction of the recovery to be due to temperature dependence and the remainder to be due to dependence upon a structural parameter such as free volume. The fractional contribution of temperature and structure is generally chosen so as to fit experimental data. We will now briefly outline the approaches of several investigators to this problem.

Moynihan et al. [68] assumed that τ follows the Twyman viscosity relationship

$$\eta = A \exp(-BT) \tag{33}$$

to derive the equation

$$\tau = A \exp(-BT)\exp(-C(T^* - T)) \tag{34}$$

where A, B, and C are constants and T^* is the fictive temperature. The fictive temperature is defined as that temperature at which the material would be at equilibrium if cooled or heated very rapidly to it [72]. Thus, the difference between the fictive temperature and the actual temperature is a measure of the departure of the material from

equilibrium. The fictive temperature may be determined from macroscopic properties by [73]:

$$T^* - T = \frac{\delta}{\Delta\alpha} = \frac{\delta_H}{\Delta C_p} \tag{35}$$

Narayanaswamy [67] used a similar approach to obtain the equation

$$\tau = A' \exp(x\, E_a/RT)\exp((1-x)E_a/RT^*) \tag{36}$$

where A' and E_a are constants, and x is a partition parameter ($0 < x \leq 1$) characterizing the pure contribution of temperature to the relaxation or retardation times. Further manipulation leads to

$$\tau = A' \exp(-\theta T)\exp(-(1 - x)\theta(T^* - T)) \tag{37}$$

where

$$A = A' \exp(2E_a/RT_g) \tag{38}$$

$$B = E_a/RT_g^2 = \theta \tag{39}$$

and

$$C = (1 - x)\theta \tag{40}$$

and A, B, and C refer to the constants in the Moynihan equation.

Kovacs et al. [2] have derived an equation of the same form as the previous two from the WLF equation. Their final equation is

$$\tau(T,\delta) = \tau_g \exp\left(\frac{-b\delta/f_T}{f_T + \delta}\right) \cdot \exp\left(\frac{-(b/f_g)(T-T_g)}{(f_s/\alpha_f)+T-T_g}\right) \tag{41}$$

where τ_g is the retardation time in equilibrium at T_g and the subscript T indicates the value at temperature T. Further development by

Kovacs et al. [2] suggested the use of a hybrid equation of the form

$$\tau(T,\delta) = \tau_g \exp\left(\frac{-b\delta f_T'^{-1}}{f_T' + \delta}\right) \exp\left(\frac{E(T_g - T)}{RTT_g} + \frac{b/f_g'(T_g - T)}{(f_g'/\Delta\alpha) + T - T_g}\right) \tag{42}$$

where the pure temperature dependence of τ is related to an activation process and the contribution of structure is related to free volume using the WLF equation.

Adam and Gibbs [15] derived an expression for τ from molecular kinetic considerations:

$$\tau = A'' \exp\left(\frac{\varepsilon}{TS_c}\right) \tag{43}$$

where ε is a constant energy and S_c is the conformational entropy. For enthalpy recovery near T_g,

$$\tau'(T,\delta_H) = \tau_g' \exp\left(\frac{\varepsilon}{TS_c} - \frac{\varepsilon}{T_g S_g}\right) \tag{44}$$

where $\delta_H = (H - H_\infty)/H_\infty$, τ_g' is the enthalpy retardation time at T_g, and $S_g = \Delta C_p \ln (T_g/T_\beta)$. It can be shown [15] that this equation leads, as a first approximation, to the WLF equation for the case of equilibrium. For nonequilibrium, there is the additional factor $\exp(-\varepsilon\delta_H/S_{C,T}^2 T^2)$.

All of the expressions considered above involve three material parameters, e.g., A', θ, and x. The pre-exponential factors A' may be eliminated by referring τ to its equilibrium value at T_g, and θ may be determined from the temperature dependence of appropriate rate parameters in the transition range.

Hutchinson and Kovacs [73] and O'Reilly [74] have approached the problem of separating the relative contributions of temperature and structure to recovery kinetics by monitoring the variations in T_g or T_{max} (that temperature at which $\alpha = dV/dT$ passes through a maximum on heating) with heating rate. In general, as the relative contribution of structure to the relaxation or retardation times increases, then $dT_{max}/d(\log|q|)$ becomes increasingly greater than $dT_g/d(\log|q|)$. For pure temperature dependence, the two derivatives are approximately equal. They have achieved good results, and this appears to be a promising area for future research.

If isothermal relaxation involved a single retardation time, the relative contribution of structure to τ could be found from τ_{eff} plots since $\tau = \tau_{eff}$ in this case. Such a plot is shown in Figure 33. For the models considered above this gives

$$\left(\frac{\partial \ell n\ \tau_{eff}^{-1}}{\partial \delta}\right)_{1,T} = \left(\frac{\partial \ell n\ \tau^{-1}}{\partial \delta}\right)_T = \frac{C}{\Delta\alpha}$$

$$= \frac{(1-x)\ E_a}{\Delta\alpha R(T^{*2})} = \frac{b}{(f_T + \delta)^2} = \frac{\varepsilon \Delta C_p}{S_{c,T}^2 T^2} \qquad (45)$$

where the subscript 1 signifies a single retardation time at temperature T. This suggests that near equilibrium the log (τ_{eff}^{-1}) vs. δ curves always have a finite positive slope whether δ is positive or negative. Thus, all single parameter models are incompatible within a linear range of δ. The theoretical variation of log (τ_{eff}) with δ at T_r-S° according to equations (41) and (42), is given by

$$\log (\tau_{eff})_{1,T} = \log \tau_T - \frac{b\delta/2.303\ f_T}{f_T + \delta} \qquad (46)$$

This prediction, shown in Figure 32 as a dotted line, is seen to be drastically different than the experimental results at T_r-5°.

Kovacs et al. [2, 69-71] have found that by treating the problem as a distribution of retardation or relaxation times, the discrepancies seen in the results of the other models are overcome. They assume that there is a particular mode of molecular motion which controls a specific fraction δ_i of the total recoverable free volume δ. It is further assumed that variations in δ_i can only occur through the i^{th} retardation mechanism. Thus, δ_i remains unaffected by other retardation mechanisms. Although this is not likely to be entirely true, such an assumption simplifies the mathematics greatly, and leads to results that are much better than those offered by previous models. Each relaxation, in isothermal recovery, follows the equation

$$\frac{d\delta_i}{dt} = - \frac{\delta_i}{\tau_i(\delta)} \qquad (47)$$

Each of the retardation times, $\tau_i(\delta)$, is dependent upon the total free volume of the system at any time and temperature.

Aklonis and Kovacs [71] used this approach to obtain the log (τ_{eff}) vs. δ plot shown in Figure 32. To obtain this plot they used a typical set of material parameters, the distribution function shown in Figure 33 and the following equation derived by Toole [72]

$$\tau_i(\delta,T) = \tau_{i,r} \exp(-\theta(T-T_r)) \exp\left(-(1-x)\frac{\partial\delta}{\Delta\alpha}\right) \qquad (48)$$

All of the plots depicting glassy behavior in Figures 31 and 32 were obtained in this manner. Again, τ_{eff} behavior resulting from the distribution of retardation or relaxation times is clearly quite different than that predicted by models using a single retardation or relaxation time. But how do these predictions compare with experiment? Figure 34 compares the experimental and theoretical τ_{eff} behavior of poly(vinyl acetate). The success of the theory in predicting the experimental τ_{eff} behavior is rather striking. Again, the τ_{eff} behavior predicted by assuming a single retardation or relaxation time is shown by the dotted line on Figure 34a. Its failure in predicting the experimental τ_{eff} is obvious.

There is one serious discrepancy between the experimental and theoretical plots in Figure 34 [2]. As $|\delta|$ approaches zero for the experimental expansion isotherms determined at the same temperature, different limiting values for τ_{eff} are reached. However, for the corresponding theoretical plots a single value of τ_{eff} is reached. The failure of the experimental expansion isotherms to reach the same equilibrium τ_{eff} value for recovery at the same temperature indicates that the equilibrium states are not determined by temperature and pressure alone as assumed by all of the models, but depend also on the previous thermal history of the material. Kovacs, et al. [2] suggest that this effect is due to structural changes which contribute negligibly to volume. A second explanation to this problem is given by Aklonis in this issue.

Thus, definite progress is being made in developing phenomenological models to quantitatively describe the recovery behavior of glassy polymers submitted to stepwise and/or continuous changes in temperature. The development of a model which accounts for both temperature and structural contributions while utilizing a distribution of retardation or relaxation times is an important advance.

C. A Molecular Approach

All of the theories which we have considered thus far utilize thermodynamics, physical modeling, or a combination of both in an attempt to describe the nonequilibrium behavior of glassy polymers. As we have seen, these approaches have yielded various degrees of success. Until recently, there has been little effort to relate molecular behavior to the observed macroscopic property behavior. Clearly, however, to obtain a complete understanding of nonequilibrium behavior in polymers, such a correlation must be made.

Robertson [75-78] has approached the problem of relating molecular structure to nonequilibrium behavior by suggesting that the recovery process can be described by the approach of the conformational degrees of freedom of the polymer backbone toward equilibrium. Thermal fluctuations cause variable free volume environments, and conformational changes occur only in regions of sufficient free volume. Thus, the distribution of retardation or relaxation times results from these variable free volume environments.

Specifically, Robertson has proposed a simple but informative model in which there are two possible states, cis and trans, and in which the bonds are equal in length and the bond angles are 90°. In addition, atom

overlaps are allowed since the changes in conformational populations are not strongly dependent on the allowed conformational states. The model describes a set of conformational transformations involving the fewest number of backbone atoms (five) and which are likely to contribute to volume or enthalpy recovery. It is assumed that the rate of conformational changes is dependent upon the fractional free volume within the environment of the transforming segment in the same way that the macroscopic recovery depends on the average free volume.

Robertson further assumes that the fractional free volume consists of both the actual free space and the ability to acquire free volume locally from coordinated motion. The rate of conformational change of a five-bond segment is given by α^a/τ. In this expression, τ is given by the WLF equation and represents the barrier to internal rotation as seen by a trans state. The symbol α is the factor by which the rate of rotation of a bond in a cis state is increased as compared to a bond in a trans state due to the energy difference ΔE between the cis and trans states, and is given by

$$\alpha = \exp(\Delta E/RT) \tag{49}$$

The symbol a represents rotating bonds initially in cis states. The rate of environmental change, which also influences the rate of conformational change, is given by

$$\lambda = A' \tau_g^{-1} \exp\left\{-B\left(\frac{z}{f + (z-1) f_{av}} - \frac{1}{f_g}\right)\right\} \tag{50}$$

where f is the fractional free volume of the changing environment, f_{av} is the average fractional free volume of the system, f_g is the average

fractional free volume at the glass transition, and z is an adjustable parameter with a value suggested to be near 12.

The effect of thermal fluctuations upon the fractional free volume is given by

$$f_{rms} = (\Delta\beta\, kT/V)^{\frac{1}{2}} \tag{51}$$

which is the root-mean-squared fluctuation. In this equation, $\Delta\beta$ is the difference in the liquid and glass compressibilities, k is Boltzmann's constant, and V is the volume of the relaxation environment. Using a plausible set of parameters, Robertson determined the f_{rms} for polystyrene at the glass transition to be 0.017. Compared to a fractional free volume of 0.028 for polystyrene at T_g, it is clear that the contribution of thermal fluctuations to volume fluctuations is significant. Thus, it is viewed that these fluctuations cause a distribution in free volume and hence a distribution of retardation or relaxation times.

Since a presentation of the mathematical methods utilized by Robertson is beyond the scope of this paper, we will move directly to a consideration of the very important results obtained. Calculations were performed to determine the τ_{eff} behavior of polystyrene as a function of the departure from volumetric equilibrium using a typical set of material parameters [76]. Although these results cannot be directly compared to Kovacs' [30] results for poly(vinyl acetate), the qualitative features of the τ_{eff} behavior are seen in Figure 36 to be quite similar to the poly (vinyl acetate) data provided the difference in the T_g's of the two polymers are taken into account. However, this model, like the phenomenological models, does not predict the dependence of equilibrium states

on previous thermal history evidenced by Kovacs' data. In spite of this shortcoming, the clear success of this molecular model in qualitatively describing the complex τ_{eff} behavior has important implications, and contributes to our understanding of the glassy state and nonequilibrium behavior.

Robertson [77,78] has also applied this technique to predict enthalpy recovery behavior with some rather interesting results. He has suggested, based on this work, that use of differential scanning calorimetry to monitor physical aging may lead to uncertainties in interpretation of data, including (1) underestimation of the conformational heat capacity, (2) incorrect comparison of samples aged at different temperatures, and (3) uncertainty of the quenched state. With regard to this latter problem, Robertson's results suggest that the quenched state is dependent upon the temperature above T_g from which the sample is cooled. This speculation, however, has no direct support at this time.

V. FINAL COMMENTS

Within this paper, we have attempted to present an unbiased overview of recent work dealing with thermodynamic nonequilibrium in glassy polymers. It is also hoped that a by-product of this paper will be to acquaint those not already familiar with this area with the principles of nonequilibrium behavior and also with an appreciation of the need to be aware of this effect when utilizing polymer materials in engineering applications.

It is clear that significant advances have been realized in recent years by both experimental and theoretical approaches. These efforts have provided a better understanding of nonequilibrium behavior and its

influence on the properties of various types of polymer systems. With the current active state of research in this area, there are certain to be forthcoming even more important advances as some of those given within the oncoming papers in this special issue of Polymer Engineering and Science.

ACKNOWLEDGEMENT

The authors gratefully acknowledge the financial assistance from the Office of Naval Research, NASA/Langley and ICI Americas, which assisted in the support of this review.

REFERENCES

1. S. E. B. Petrie, in "Polymeric Materials: Relationships Between Structure and Mechanical Behavior," Am. Soc. for Metals, Metal Park, OH (1975).

2. A. J. Kovacs, J. M. Hutchinson, and J. J. Aklonis, in "The Structure of Non-Crystalline Materials," P. H. Gaskell, Ed., Taylor and Francis, London (1977).

3. L. C. E. Struik, "Physical Aging in Amorphous Polymers and Other Materials," Elsevier, New York (1978).

4. I. M. Ward, "Mechanical Properties of Solid Polymers," Wiley-Interscience, New York (1971).

5. J. D. Ferry, "Viscoelastic Properties of Polymers," Wiley & Sons, New York (1971).

6. R. B. Bird, W. E. Stewart, and E. N. Lightfoot, "Transport Phenomena," Wiley & Sons, New York (1960).

7. W. Wrasidlo, Adv. Polym. Sci. 13, 1 (1974).

8. M. L. Williams, J. Phys. Chem. 59, 95 (1955).

9. M. L. Williams, R. F. Landel, and J. D. Ferry, J. Am. Chem. Soc. 77, 3701 (1955).

10. A. K. Doolittle, J. Appl. Phys. 22, 1471 (1951).

11. M. H. Cohen and D. Turnbull, J. Chem. Phys. 31, 1164 (1959).

12. D. Turnbull and M. H. Cohen, J. Chem. Phys. 34, 120 (1961).

13. J. H. Gibbs and E. A. diMarzio, J. Chem. Phys. 28, 373 (1958).

14. J. H. Gibbs and E. A. diMarzio, J. Chem. Phys. 28, 807 (1958).

15. G. Adam and J. H. Gibbs, J. Chem. Phys. 43, 139 (1965).

16. P. Ehrenfest, Proc. Kon. Akad. Wetensch. Amsterdam 36, 153 (1933).

17. G. Rehage and W. Borchard, in "The Physics of Glassy Polymers," Wiley & Sons, New York (1973).

18. S. L. Rosen, "Fundamental Principles of Polymeric Materials," Barnes & Noble, New York (1971).

19. E. Ito, K. Yamamoto, Y. Kobayashi, and T. Hatakeyama, Polymer 19, 39 (1978).

20. R. S. Moore and J. K. O'Loane, Org. Coat. and Plast. Chem. 39, 224 (1978).

21. L. C. E. Struik, Ann. N. Y. Acad. Sci. 279, 78 (1976).

22. L. C. E. Struik, Rheol. Acta 5, 303 (1976).

23. S. Matsuoka, H. E. Bair, S. S. Bearder, H. E. Kern, and J. T. Ryan, Polym. Eng. Sci. 18, 1073 (1978).

24. Z. H. Ophir, J. A. Emerson and G. L. Wilkes, J. Appl. Phys. 49, 5032 (1978).

25. L. C. E. Struik, Polym. Eng. Sci. 18, 799 (1978).

26. S. Y. Pusatcioglu, J. C. Hassler, A. L. Fricke and H. A. McGee, J. Appl. Polym. Sci. 25, 381 (1980).

27. L. J. Broutman and S. M. Krishnakumer, Polym. Eng. & Sci. 16, 74 (1976).

28. G. Goldbach and G. Rehage, Rheol. Acta 6, 30 (1967).

29. J. E. McKinney and M. Goldstein, J. Res. Nat. Bur. Stand., A, 78, 331 (1974).

30. A. J. Kovacs, Fortschr. Hochpolym. Forsch. 3, 394 (1963).

31. S. E. B. Petrie, J. Polym. Sci. A-2 10, 1255 (1972).

32. S. E. B. Petrie, in "Physical Structure of the Amorphous State," G. Allen and S. E. B. Petrie, Eds., Marcel Dekker, New York (1977).

33. Yu A. Sharanov and M. V. Volkenshtein, in "The Structure of Glasses," Vol. 6, E. A. Porai-Koshits, Ed., Consultants Bureau, New York (1966).

34. V. Frosini, G. Levita, and A. Marchetti, Journees de Calorimetrie et d'Analyse Thermique IX-A, B5-35 (1978).

35. V. Frosini, A. Marchetti, and E. Butta, La Chimica e l'Industria 59, 415 (1977).

36. I. G. Brown, R. E. Wetton, M. J. Richardson and N. G. Savill, Polymer 19, 659 (1978).

37. R. M. Mininni, R. S. Moore, J. R. Flick and S. E. B. Petrie, J. Macromol. Sci. B8, 343 (1973).

38. J. H. Golden, B. L. Hammant, and E. A. Hazell, J. Appl. Polym. Sci. 11, 1571 (1967).

39. D. G. LeGrand, J. Appl. Polym. Sci. 13, 2129 (1969).

40. K. Neki and P. H. Geil, J. Macromol. Sci. 8, 295 (1973).

41. J. R. Flick and S. E. B. Petrie, Bull. Am. Phys. Soc. 19, 238 (1974).

42. M. R. Tant, M. S. Thesis, Virginia Polytechnic Institute and State University, Blacksburg (1979).

43. J. R. Flick and S. E. B. Petrie, company preprints.

44. K. Neki and P. H. Geil, J. Macromol. Sci. Phys. B8, 295 (1973).

45. M. Uchidoi, K. Adachi and Y. Ishida, Polym. J. 10, 161 (1978).

46. G. E. Johnson, S. Matsuoka, and H. E. Bair, Org. Coat. Plast. Chem. 38, 350 (1978).

47. A. H. Chan and D. R. Paul, Org. Coat. Plast. Chem. 39 (2), 230 (1978).

48. A. H. Chan, Ph.D. Dissertation, University of Texas, Austin (1978).

49. Z. H. Ophir, Ph.D. Dissertation, Princeton University, Princeton, NJ (1978).

50. E. S. W. Kong, M. R. Tant, G. L. Wilkes, A. K. Banthia and J. E. McGrath, Polym. Prepr. 20 (2), 531 (1979).

51. S. E. B. Petrie, private communication.

52. J. Kaiser, Makrom. Chem. 180, 573 (1979).

53. M. R. Tant and G. L. Wilkes, Polym. Prepr. 20 (2), 535 (1979).

54. M. R. Tant and G. L. Wilkes, J. Appl. Polym. Sci., submitted.

55. M. R. Tant and G. L. Wilkes, Polym. Eng. Sci., in press.

56. M. G. Wyzgoski, J. Appl. Polym. Sci. 25, 1443 (1980).

57. H. C. Booij and J. H. K. Minkhorst, Polym. Eng. Sci. 19, 579 (1979).

58. T. J. Fox and P. J. Flory, J. Appl. Phys. 21, 581 (1950).

59. R. Simha and R. F. Boyer, J. Chem. Phys. 37, 1003 (1962).

60. J. H. Gibbs, J. Chem. Phys. 25, 185 (1956).

61. J. M. Hutchinson and A. J. Kovacs, J. Polym. Sci. Polym. Phys. Ed. 14, 1575 (1976).

62. S. Matsuoka and H. E. Bair, J. Appl. Phys. 48, 4058 (1977).

63. M. J. Richardson and N. G. Savill, Polymer 18, 413 (1977).

64. A. J. Kovacs, J. Polym. Sci. 30, 131 (1958)

65. T. A. Litovitz and P. Macedo, "Proceedings International Conference on Physics of Non-Crystalline Solids," J. A. Prins, Ed., North Holland, Amsterdam (1965).

66. F. Bueche, J. Chem. Phys. 36, 2940 (1962).

67. O. S. Narayanaswamy, J. Am. Ceram. Soc. 54, 491 (1971).

68. M. A. DeBolt, A. J. Easteal, P. B. Macedo, and C. T. Moynihan, J. Am. Ceram. Soc. 59, 16 (1976).

69. J. M. Hutchinson, J. J. Aklonis, and A. J. Kovacs, Polym. Prepr. 16(2), 94 (1975).

70. A. J. Kovacs, J. J. Aklonis, J. M. Hutchinson and A. R. Ramos, J. Polym. Sci.: Polym. Phys. Ed. 17, 1097 (1979).

71. J. J. Aklonis and A. J. Kovacs, in "Contemporary Topics in Polymer Science," Vol. 3, M. Shen. Ed., Plenum, New York (1979).

72. A. Q. Tool, J. Am. Ceram. Soc. 29, 240 (1946).

73. J. M. Hutchinson and A. J. Kovacs, in "The Structure of Non-Crystalline Materials," P. H. Gaskell, Ed., Taylor and Francis, London (1977).

74. J. M. O'Reilly, Polym. Prepr. 20(1), 762 (1979).

75. R. E. Robertson, J. Polym. Sci. Polym. Symp. 63, 173 (1978).

76. R. E. Robertson, J. Polym. Sci. Polym. Phys. Ed. 17, 597 (1979).

77. R. E. Robertson, J. Polym. Sci. Polym. Lett. Ed. 17, 213 (1979).

78. R. E. Robertson, J. Appl. Phys. 49, 5048 (1978).

FIGURE CAPTIONS

Figure 1. Specific volume vs. temperature for polyvinyl acetate, measured after cooling quickly from above T_g; 0.02 h and 100 h indicate time since cooling (Kovacs [64]).

Figure 2. A qualitative representation of the free volume concept and its correlation to molecular mobility (Struik [3]).

Figure 3. Small-strain tensile creep curves of rigid PVC quenched from 90°C to 40°C and annealed at 40°C (Struik [3]).

Figure 4. Percent stress relaxation in 10 minutes for a crosslinked epoxy resin as a function of sub-T_g annealing time (Ophir et al. [24]).

Figure 5. Stress relaxation in PS with various thermal histories, but at the same strain and same temperature (Matsuoka et al. [23]).

Figure 6. The shifting of creep curves of rigid PVC quenched from 90°C to 0, 20, and 40°C. Log "a" is the shift relative to the creep curve measured one day after quench (Struik [3]).

Figure 7. The shift rate, μ, as a function of temperature for various polymers (Struik [3]).

Figure 8. Volume relaxation for atactic PS at 1 atm and 95.46 C after prior equilibration at various temperatures, T_s. V_∞ is the equilibrium volume at 95.46 C (Goldbach and Rehage [28]).

Figure 9. Pressure dependence of volume-temperature plots of the T_g interval for polyvinyl acetate (McKinney and Goldstein [29]).

Figure 10. Memory effects shown by poly(vinyl acetate) after quenching the specimen from T_0 = 40°C to T_1, at which it remained for a time t_1 before reheating to T = 30°C; (1) Intrinsic isotherm obtained by direct quenching from 40°C to 30°C, (2) T_1 = 10°C(t_1 = 160 h), (3) T_1 = 15°C (t_1 = 140 h), and (4) T_1 = 25°C(t_1 = 90 h) (Kovacs [30]).

Figure 11. Schematic diagram of enthalpy and corresponding specific heat changes for annealed (---) and unannealed (——) glasses on heating at a rate r_1 (Petrie [32]).

Figure 12. DSC scans of amorphous PET after various annealing periods at 65°C following air-quenching from 95°C. Heating rate of 10°C min^{-1} (Petrie [1]).

Figure 13. Enthalpy relaxation determined from DSC data vs annealing time for atactic PS at 92°C following air quenching to 22°C from 135°C (Petrie [1]).

Figure 14. Enthalpy relaxation determined from DSC data for atactic PS vs annealing time at various temperatures following air quenching to 22°C from about 135°C (Petrie [31]).

Figure 15. Thermal energy absorbed at the glass transition vs endothermic peak temperature for poly(phenylacrylate) (Frosini, et al. [34]).

Figure 16a. DSC traces for isothermal glass-liquid transformation of poly-(vinylbenzoate) (Frosini, et al. [34]).

Figure 16b. Time-temperature diagram for isothermal transformation of poly(vinylbenzoate) at different temperatures (Frosini, et al. [34]).

Figure 17. (a) Schematic specific volume - and (b) enthalpy - temperature curves showing the differing effects of pressure on $T_g(H)$ (little affected) and $T_g(V)$ (large changes): A, reference (1 atm); B, moderate and C, high densification pressures (Brown, et al. [36]).

Figure 18. Tensile stress-strain curves at 22°C for 5-mil amorphous PET film air quenched to 22°C from about 95°C and annealed at 51°C for the times indicated. Instron tested at an initial strain rate of 10% min^{-1} (Mininni, et al. [37]).

Figure 19. Shear storage modulus, G_1', logarithmic decrement, Δ, and enthalpy relaxation, ΔH, of quenched atactic PS vs annealing time at 92°C. G_1' and Δ were measured at 0.6 Hz (Petrie, et al. [1]).

Figure 20a. Frequency dependence of dielectric loss factors of the PVAC which were calculated by Fourier transformation of the transient currents as shown within the figure. ◐, τ_0= 1860 sec; ○, τ_0= 24400 sec; ●, τ_0= 187000 sec; ◑, τ_0= 1223000 sec. (Uchidoi [45]).

Figure 20b. Annealing time dependence of the frequency where loss becomes a maximum (Uchidoi, et al [45]).

Figure 21. Equilibrium sorption of CO_2 by polycarbonate at 35°C for samples having the thermal histories shown (Chan and Paul [47]).

Figure 22a. Stress-strain curves of a pure epoxy and two rubber modified epoxies, measured at 23°C, 10 min after quenching from above T_g (Ophir, et al. [24])

Figure 22b. Stress-strain curves of the epoxy series, measured at 23°C, 56 days after quenching above T_g (Ophir, et al. [24]).

Figure 23 Sub Tg annealing effects on the DSC traces of a epon 828 based epoxy (Ophir, et al. [24]).

Figure 24a & b. Percent stress relaxation as a function of sub-T_g annealing time for PET of the following crystallinities: (a) 0%, (b) 29%. [54]

Figure 25a & b. Stress-strain curves measured at various sub T_g annealing times for PET of the following crystallinities: (a) 0%, (b) 22%. [54]

Figure 26. Effect of mechanical deformation on the free volume or molecular mobility with log aging time. (Stouik [3])

Figure 27. Effect of a high tensile stress "pulse" of intensity σ_1 on the small strain creep properties of rigid PVC (Struik [3]).

Figure 28. Tensile stress and temperature versus tensile strain of PC at the rate of strain of 5.2×10^{-3} min^{-1} (Matsuoka and Bair [62]).

Figure 29. Schematic diagrams for heat capacity (top) and enthalpy (bottom) versus temperature for the quenched glass 1 and the annealed glass 2 (Matsuoka and Bair [62]).

Figure 30. Excess enthalpy versus time of PS annealed at 90°C , with data from Petrie [31] and Matsuoka and Bair [62]. The solid line was calculated from equation (29) (Matsuoka and Bair [62]).

Figure 31a. Typical behavior of glass formers in constant cooling rate experiments. Cooling rate = $q = dT/dt$; $v_{r,\infty}$ is the equilibrium volume at the reference temperature, T_r, and "a" is the isobaric coefficient of thermal expansion (Aklonis and Kovacs [71]).

Figure 31b. Typical behavior of glass formers in constant heating rate and constant cooling rate experiments (Aklonis and Kovacs [71]).

Figure 31c. Simple approach behavior in the glass transition region. δ is plotted versus log t at the experimental temperature $T = T_r - 5°$. For contraction $\delta > 0$ and ΔT, the temperature jump, is negative; for expansion, $\delta < 0$ and $\Delta T > 0$ (Aklonis and Kovacs [71]).

Figure 31d. Memory behavior at $T = T_r - 5°$ evoked by multiple temperature jumps. Thermal histories are shown in the insert; t_1 is the time at which the second T-jump is applied. (Alkonis and Kovacs [71]).

Figure 32. ξ_{eff} behavior at three temperatures, T_r, $T_r - 5°$ and $T_r - 10°$ for simple approach expansion and contraction experiments in the glass transition region. ΔT, the value of the temperature jump used to perturb the system from equilibrium, is listed near each curve (Aklonis and Kovacs [71]).

Figure 33. Realistic distribution of normalized instantaneous departures from equilibrium g_i as a function of recovery times τ_i. This distribution corresponds to the data shown in Figures 1 through 5 (Aklonis and Kovacs [71]).

Figure 34a & b. Experimental (a) and theoretical (b) plots of log τ_{eff} vs δ for poly(vinyl acetate) at three different temperatures. Small numbers indicate temperature from which T-jump was made (Kovacs et al. [2]).

Figure 35. Calculated relaxation times vs. extent of internal relaxation. T_1 is the sub T_g annealing temperature (Robertson [76]).

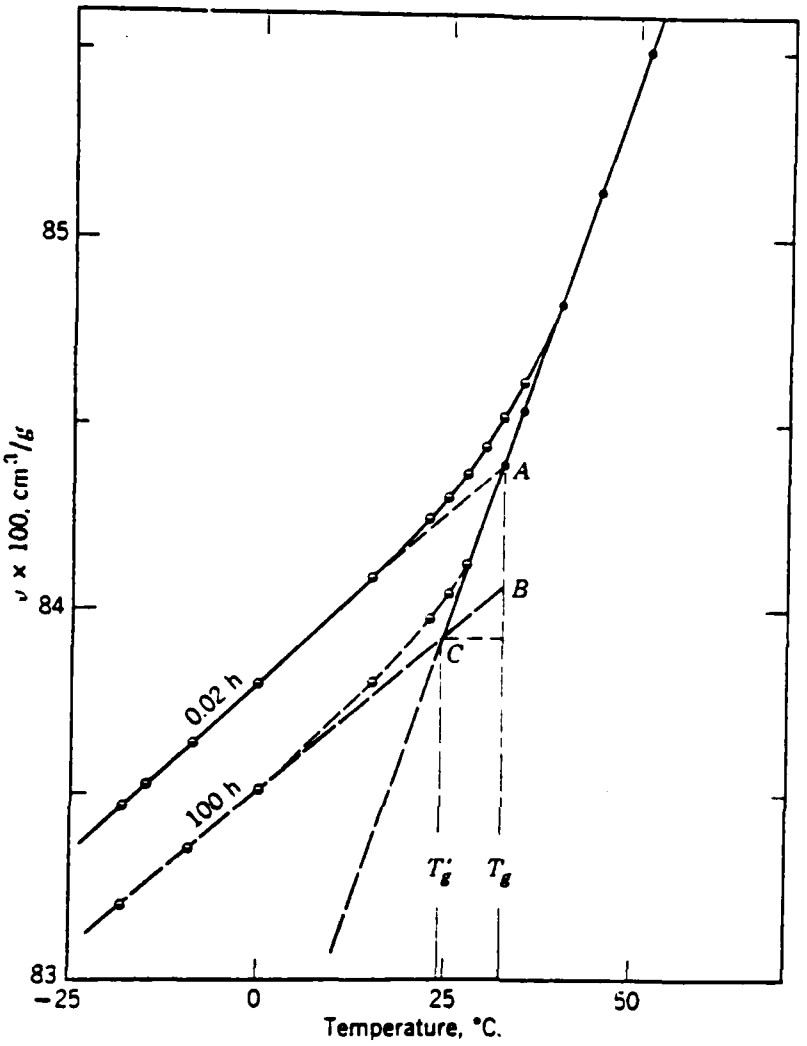

Figure 1

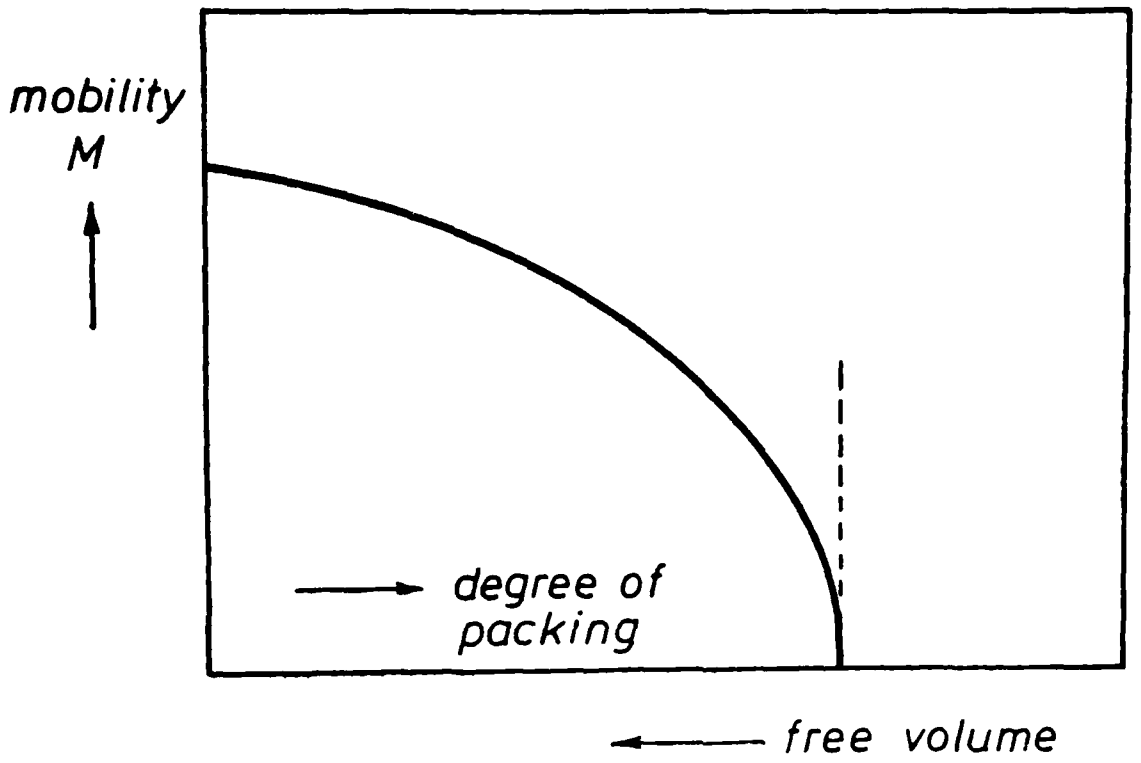

Figure 2

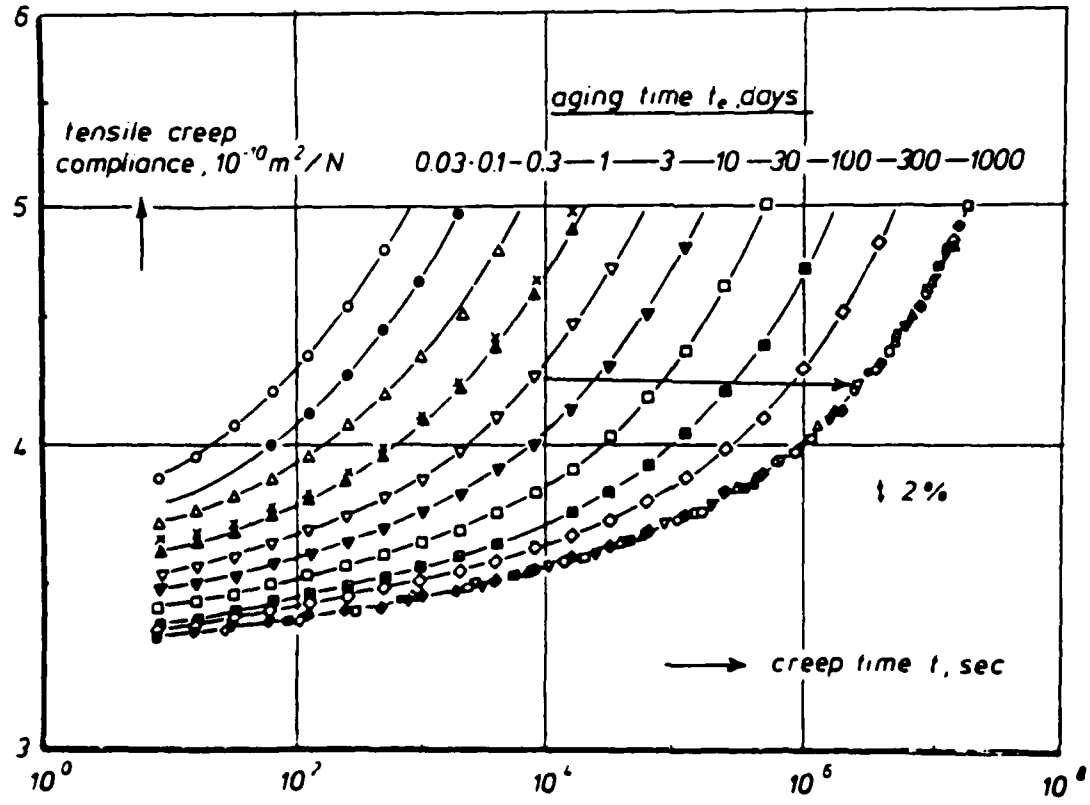

Figure 3

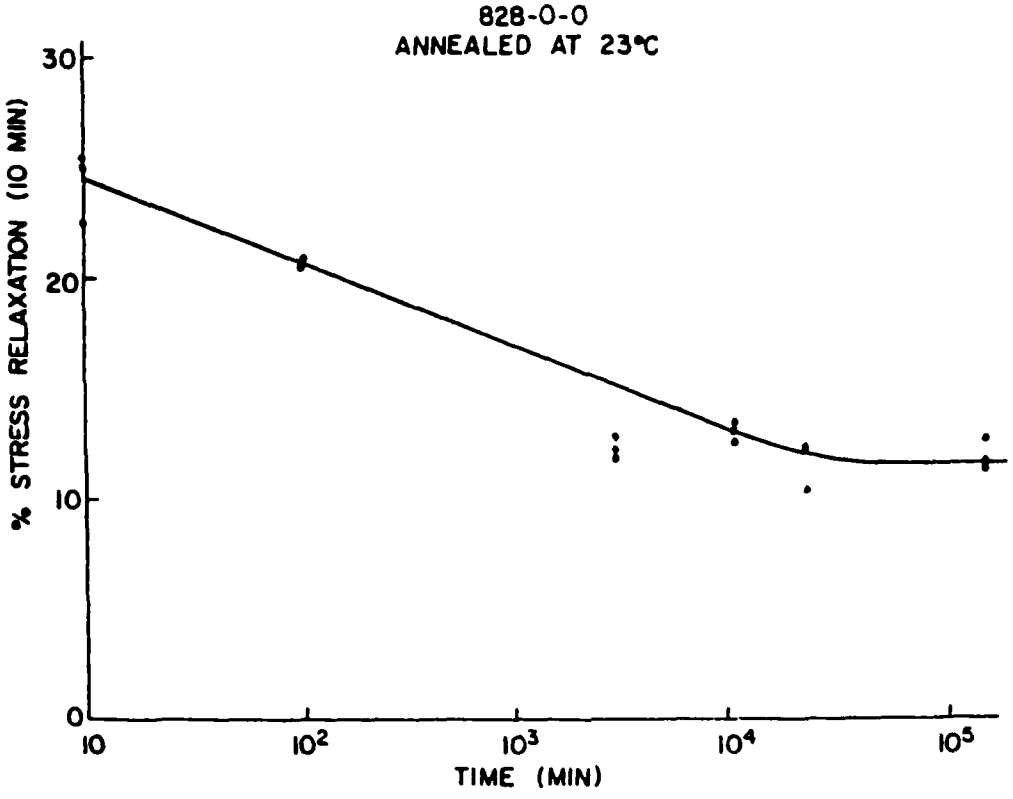

Figure 4

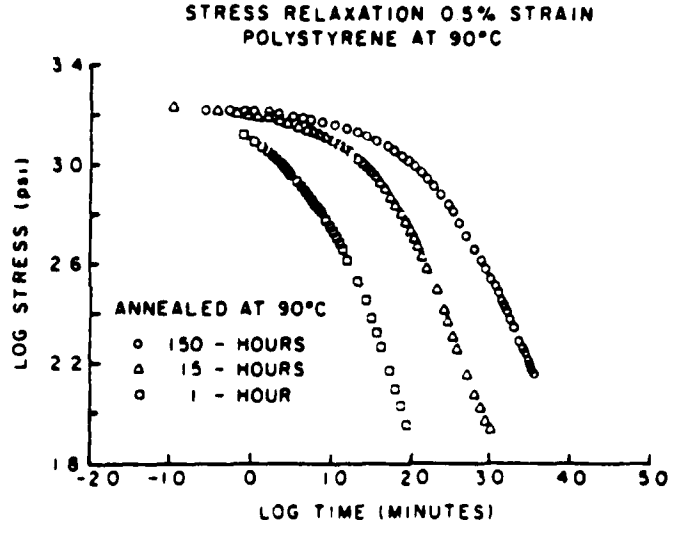

Figure 5

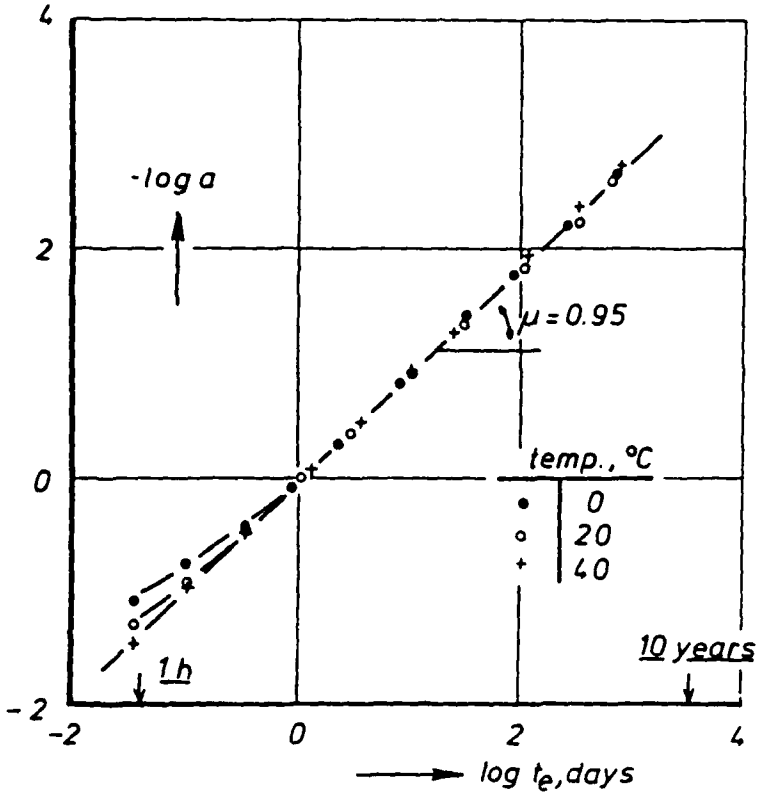

Figure 6

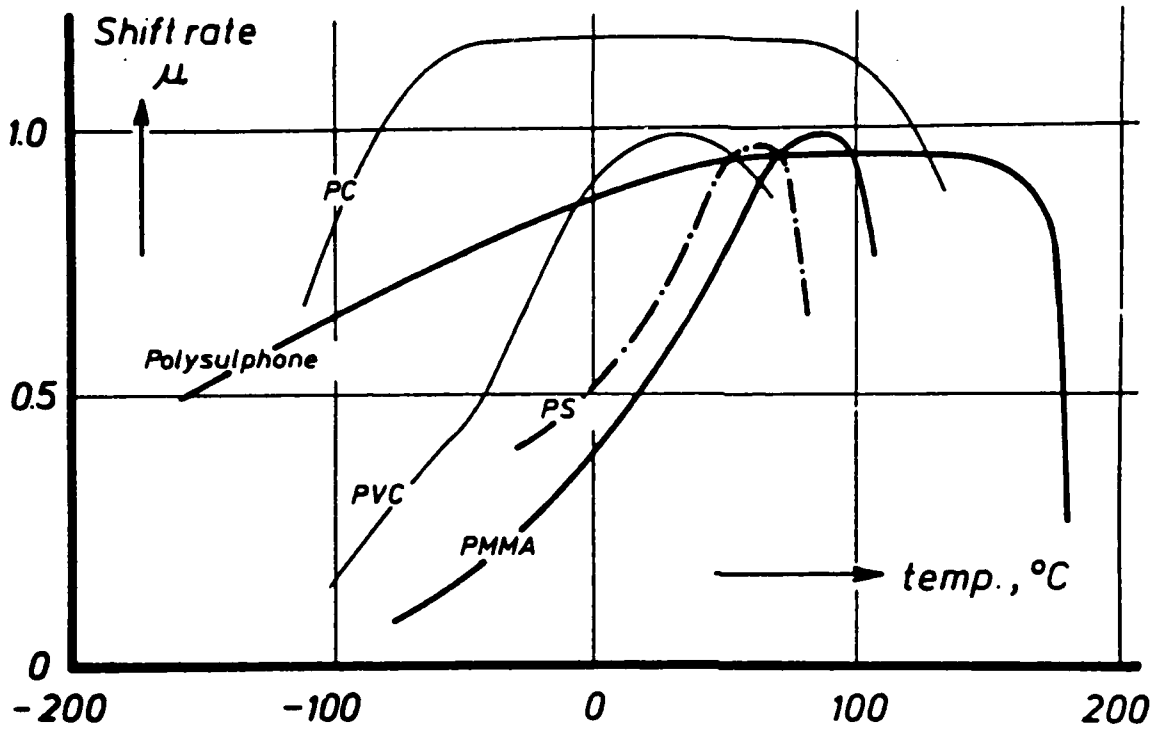

Figure 7

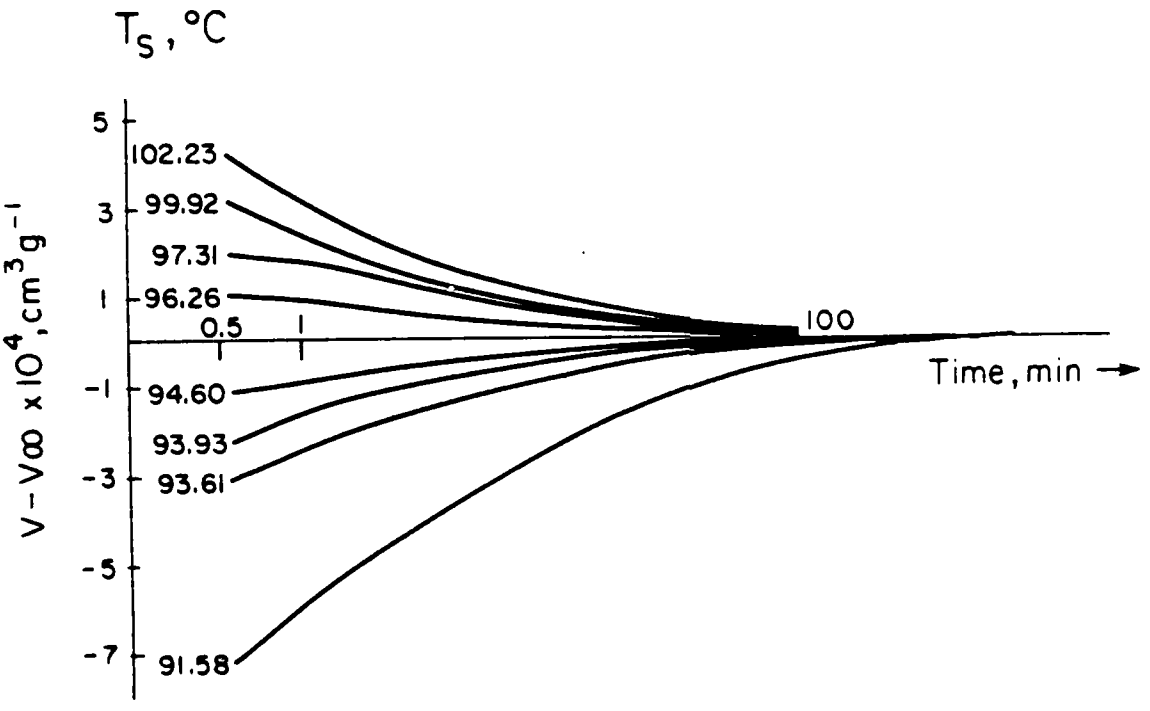

Figure 8

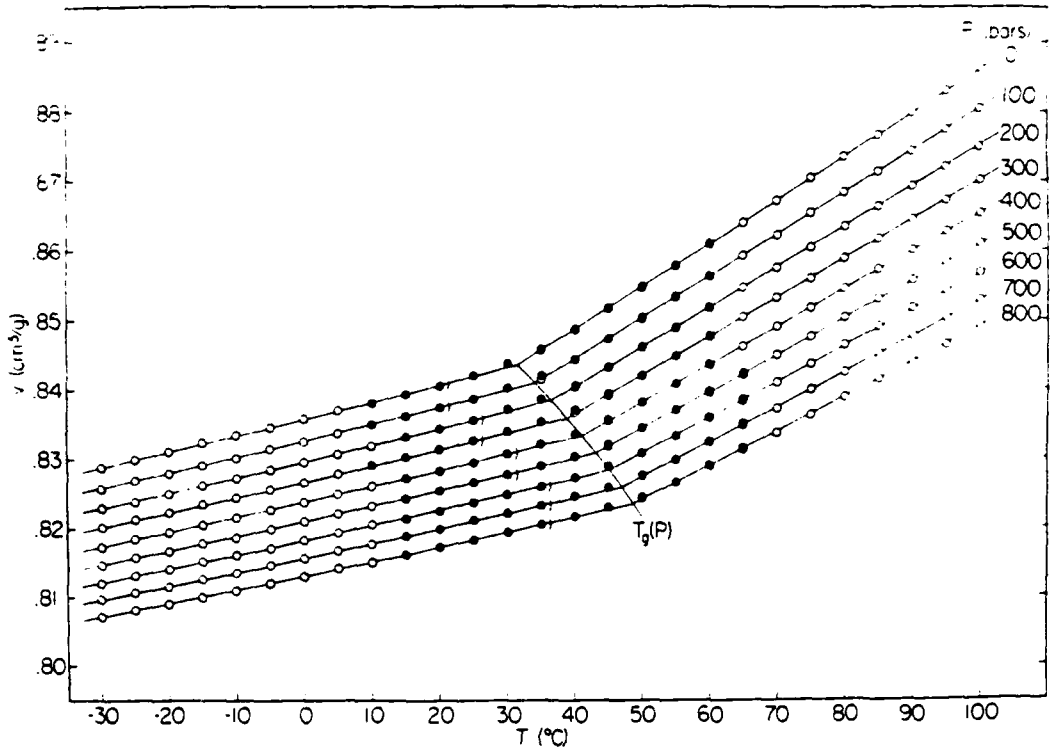

Figure 9

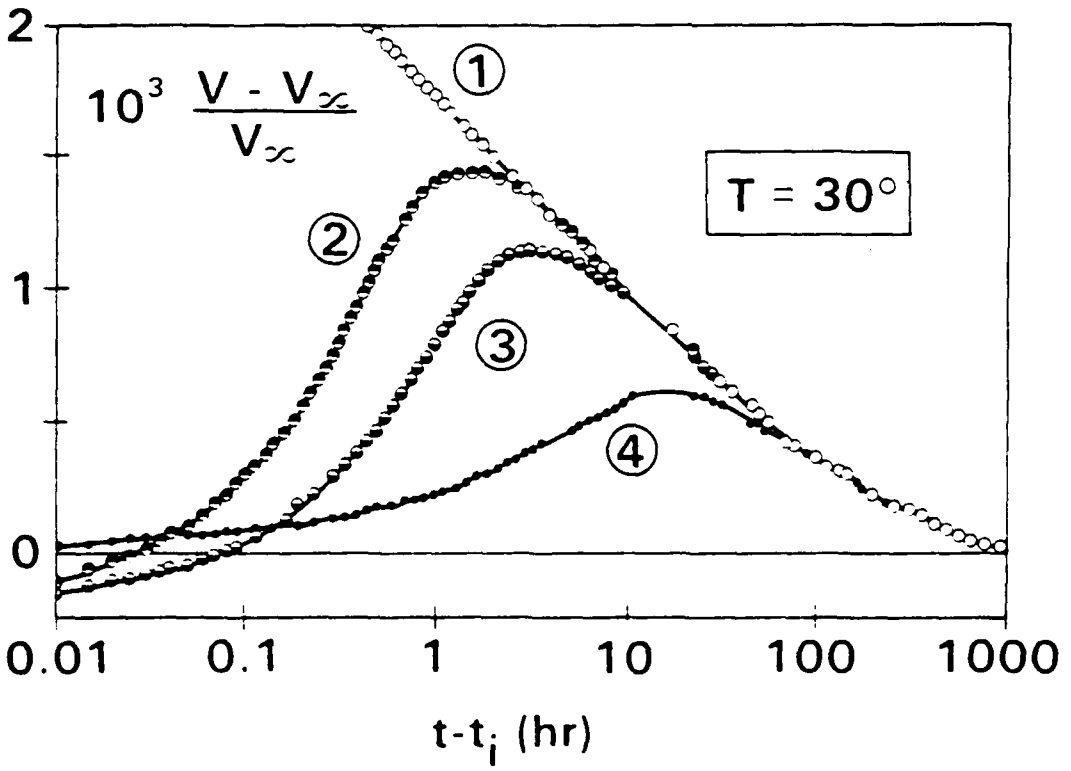

Figure 10

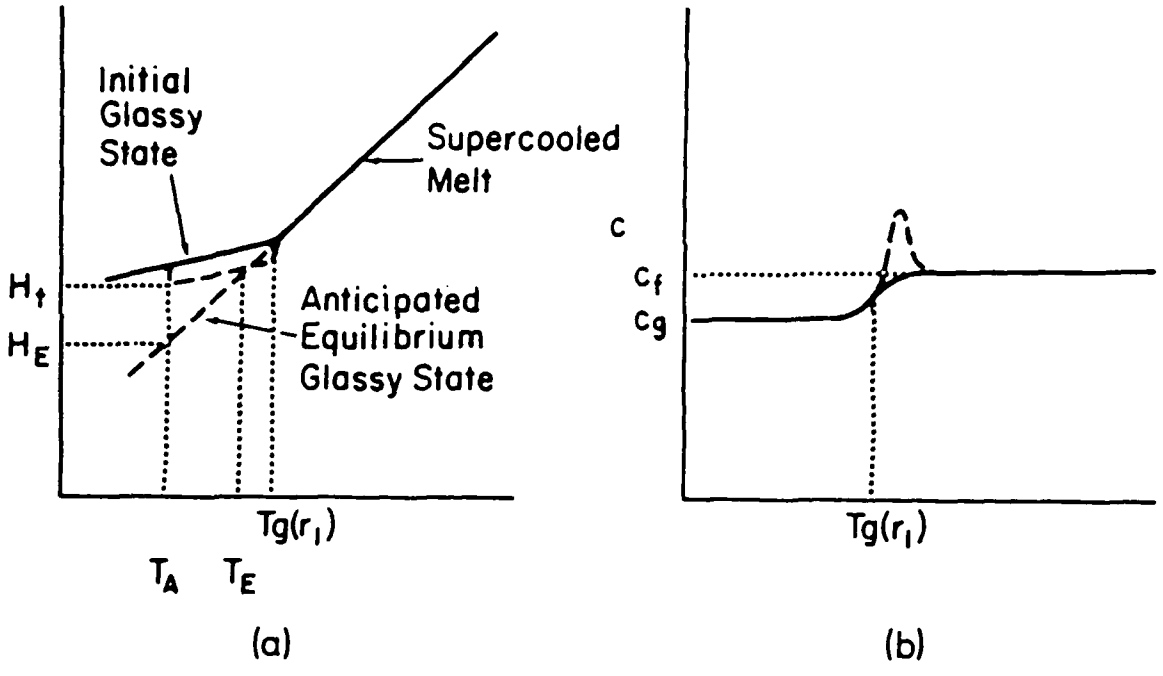

Figure 11

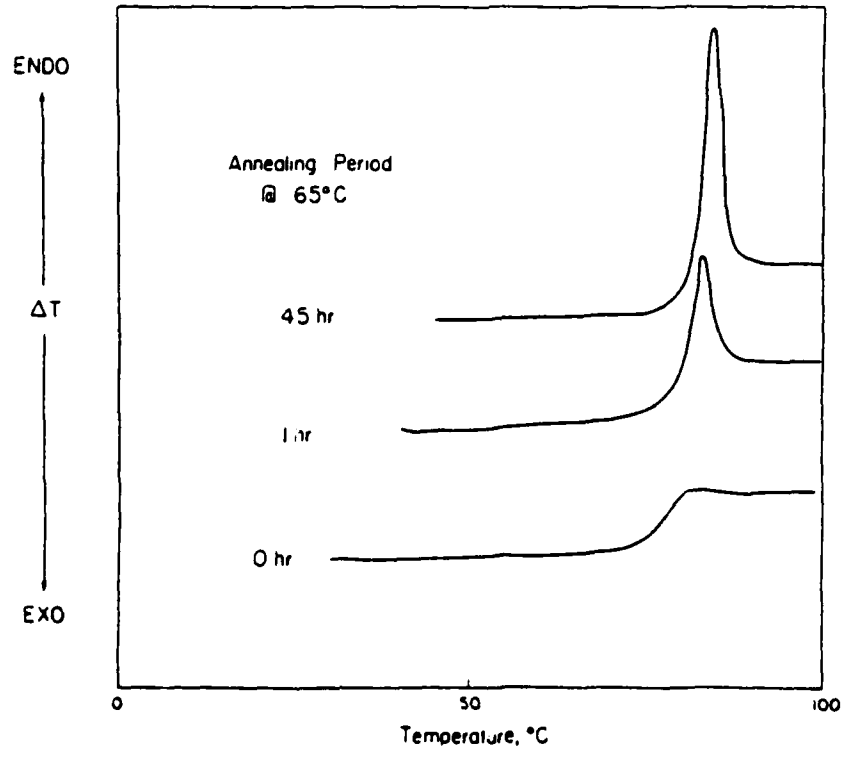

Figure 12

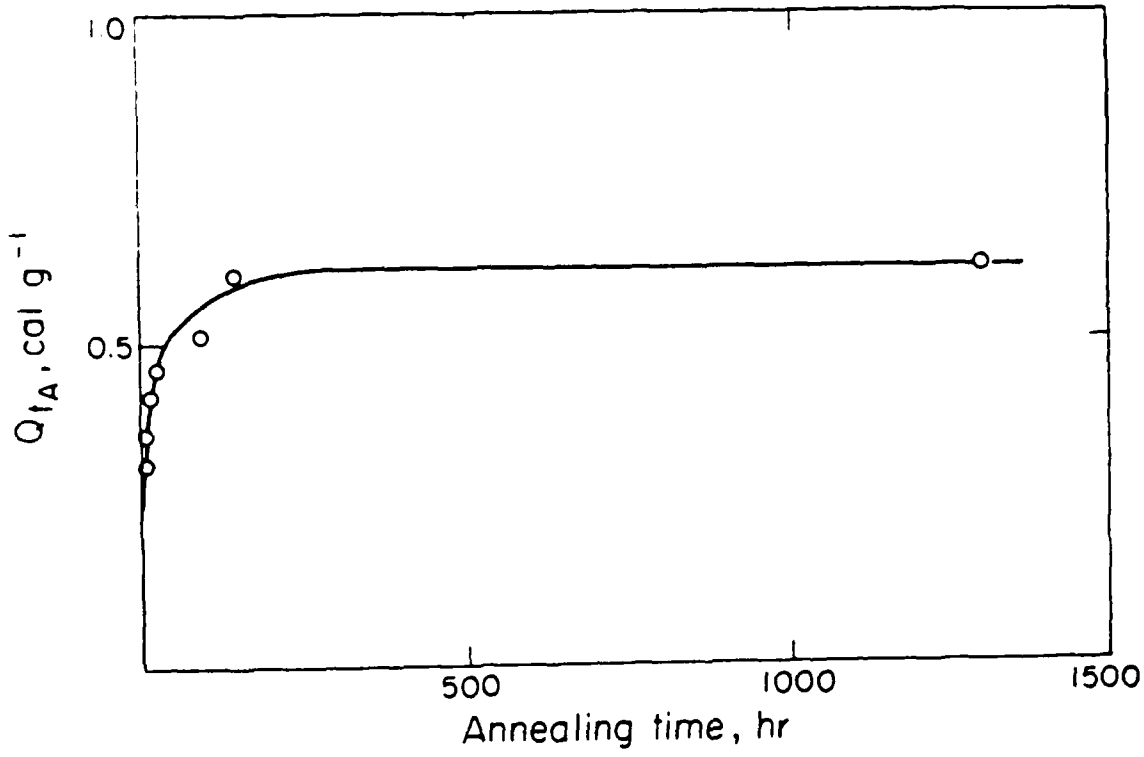

Figure 13

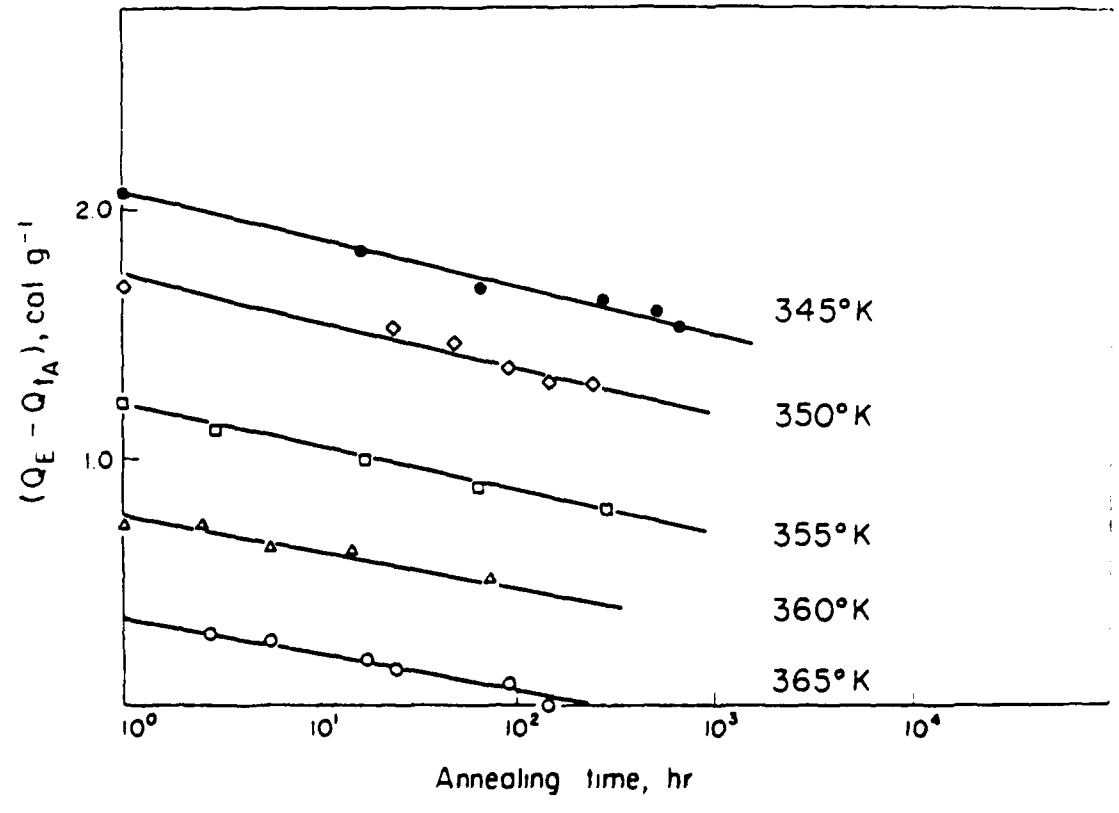

Figure 14

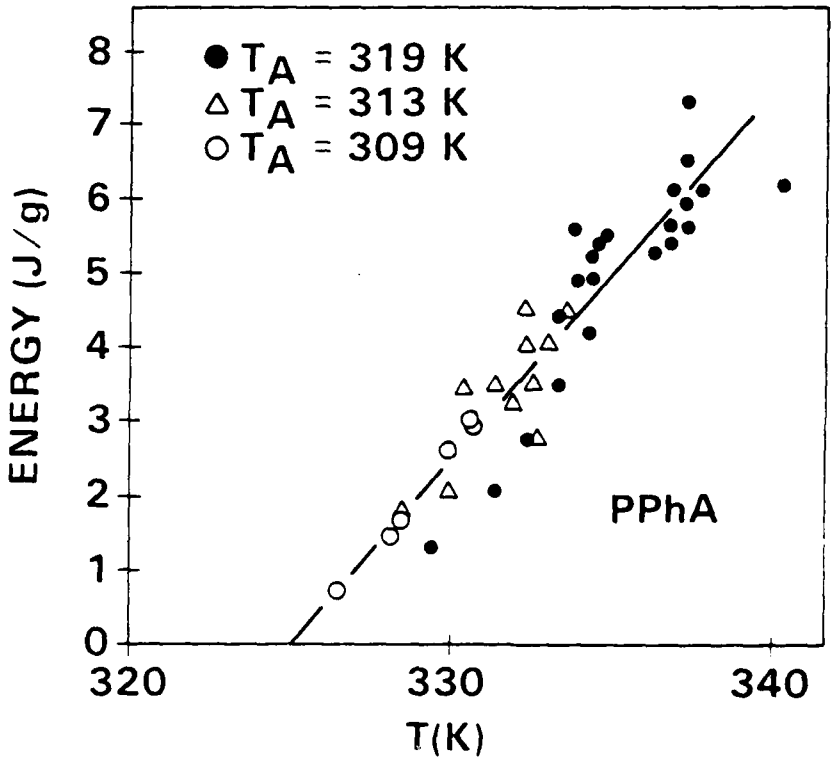
● T_A = 319 K
△ T_A = 313 K
○ T_A = 309 K
PPhA
ENERGY (J/g)
T(K)
0
1
2
3
4
5
6
7
8
320
330
340

Figure 15

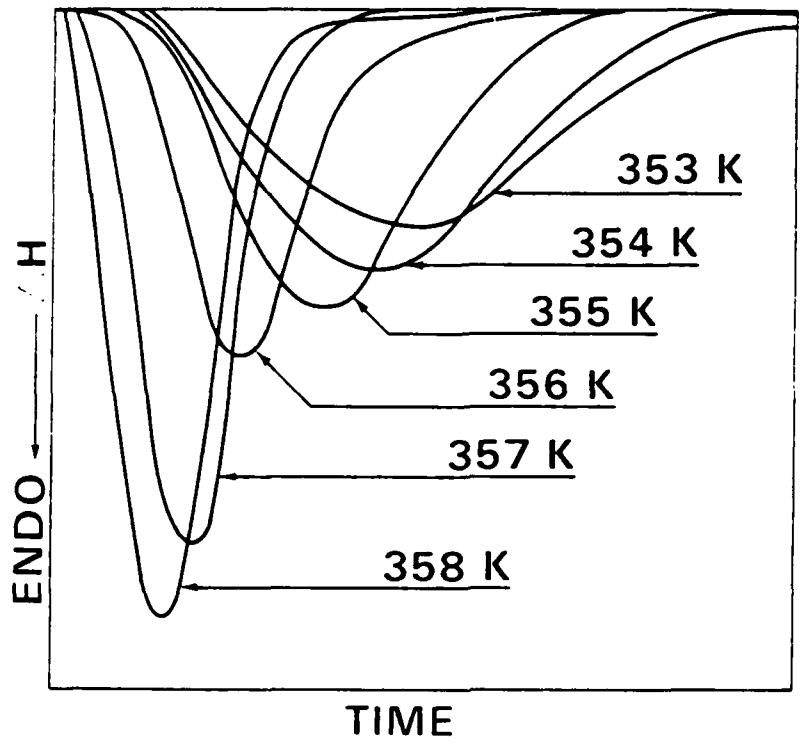

Figure 16a

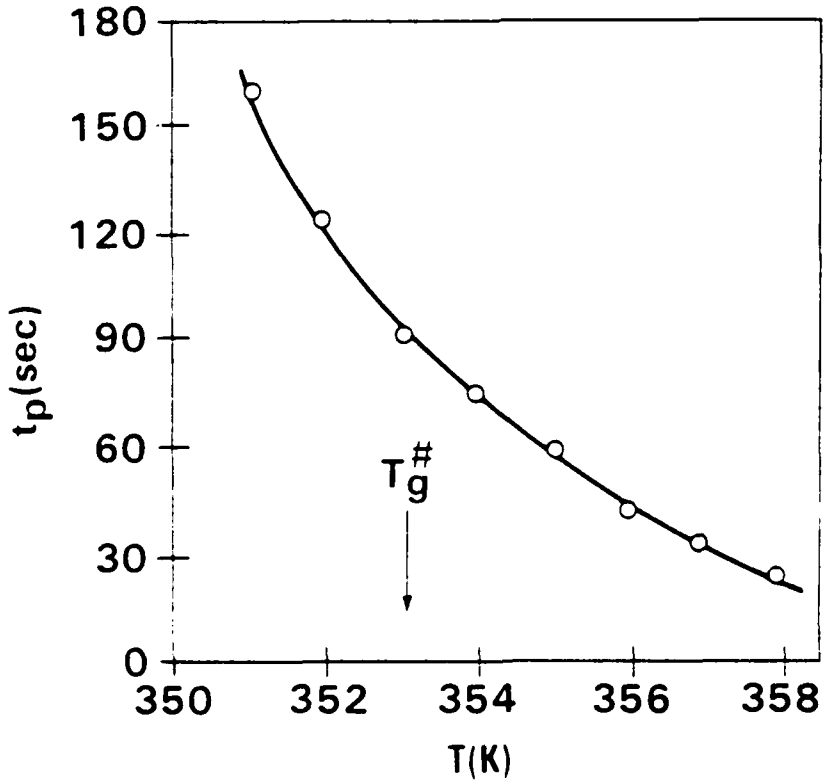

Figure 16b

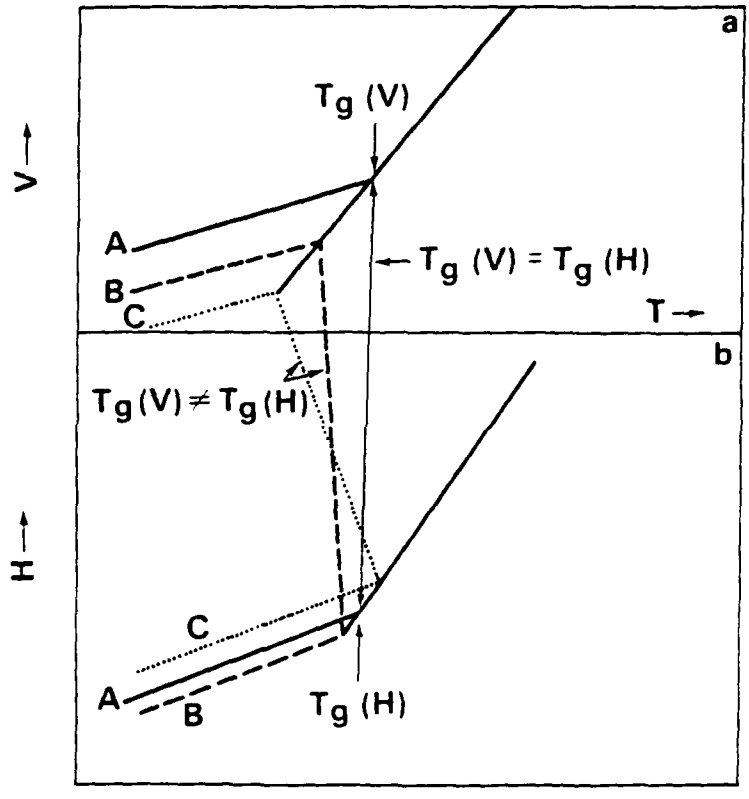

Figure 17

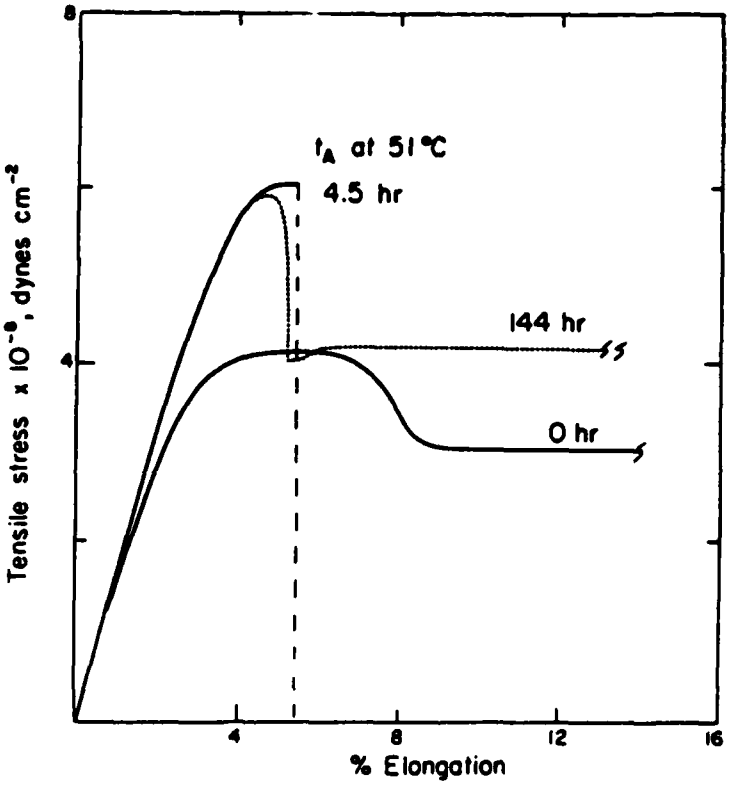
8
4
t_A at 51°C
4.5 hr
144 hr
0 hr
Tensile stress x 10^{-8}, dynes cm^{-2}
4
8
12
16
% Elongation

Figure 18

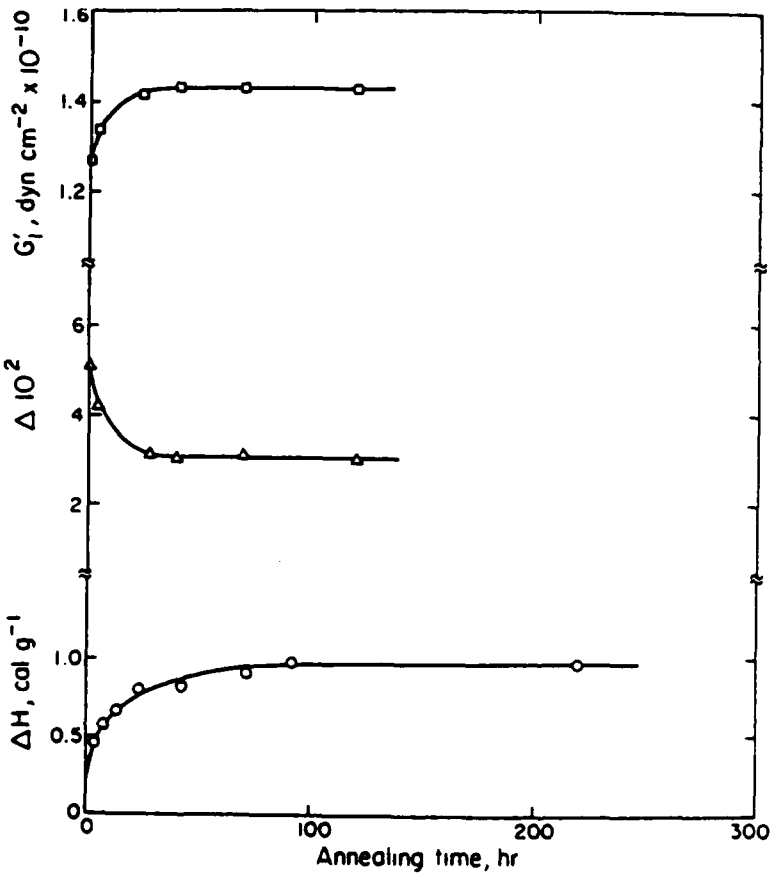
1.6
1.4
1.2
G_1', dyn cm^{-2} x 10^{-10}
6
4
Δ 10^2
2
1.0
0.5
ΔH, cal g^{-1}
0
0
100
200
300
Annealing time, hr

Figure 19

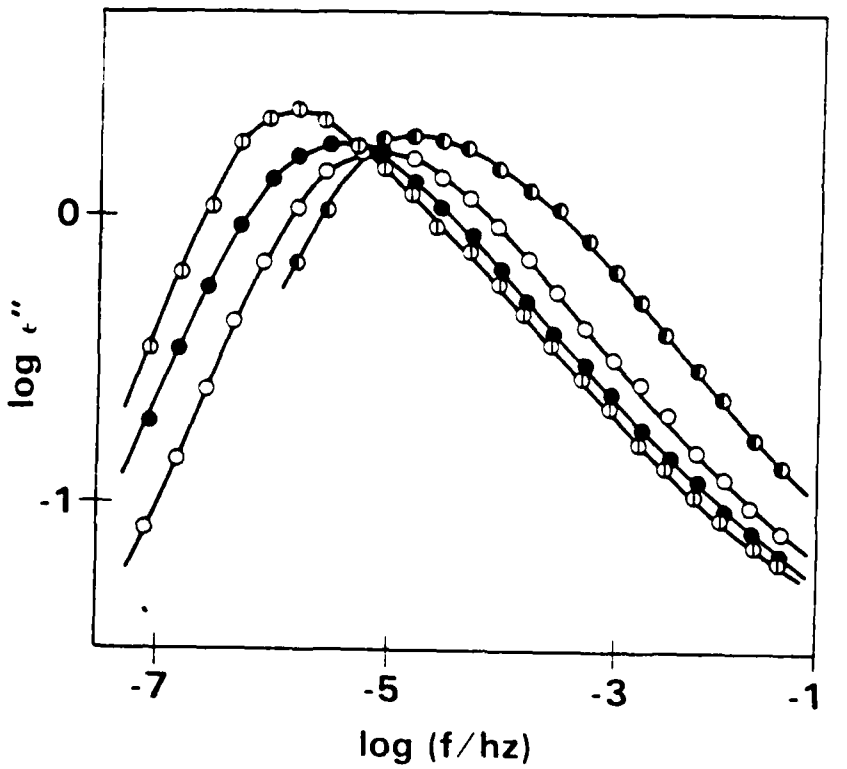

Figure 20a

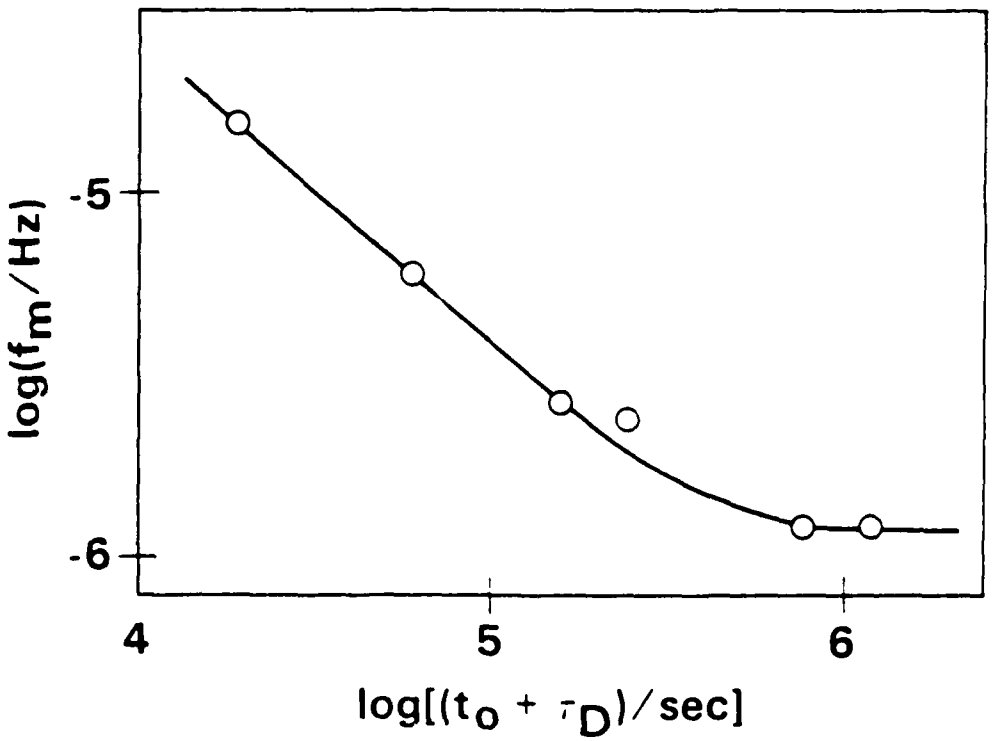

Figure 20b

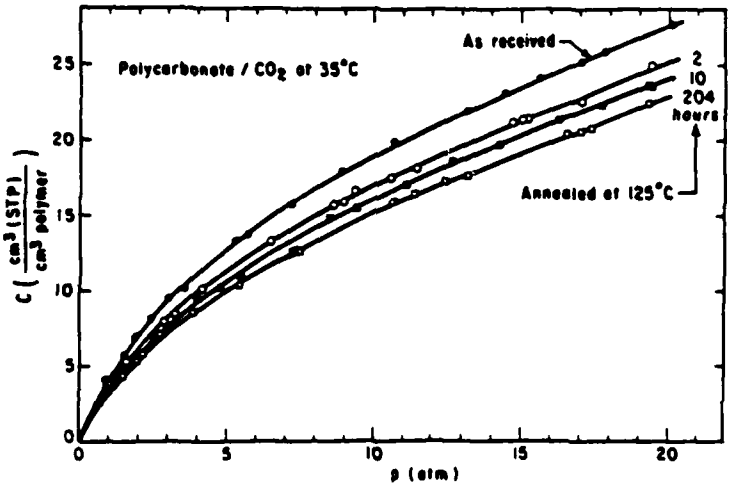
As received
2
10
204
hours
Annealed at 125°C
Polycarbonate / CO_2 at 35°C
$C\left(\frac{cm^3\,(STP)}{cm^3\ polymer}\right)$
p (atm)
0
5
10
15
20
25

Figure 21

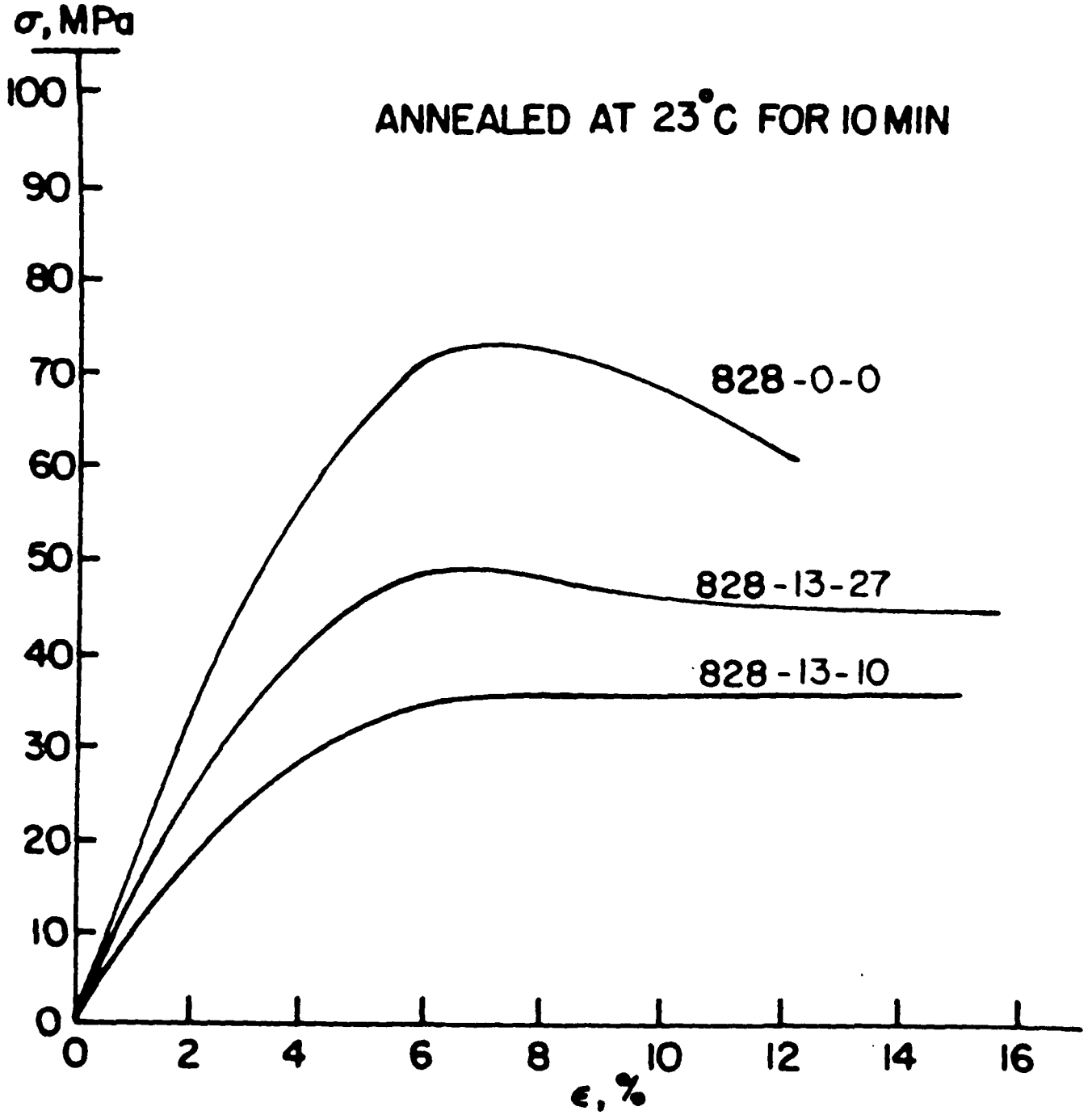
σ, MPa
100
90
80
70
60
50
40
30
20
10
0
ANNEALED AT 23°C FOR 10 MIN
828-0-0
828-13-27
828-13-10
0
2
4
6
8
10
12
14
16
ε, %

Figure 22a

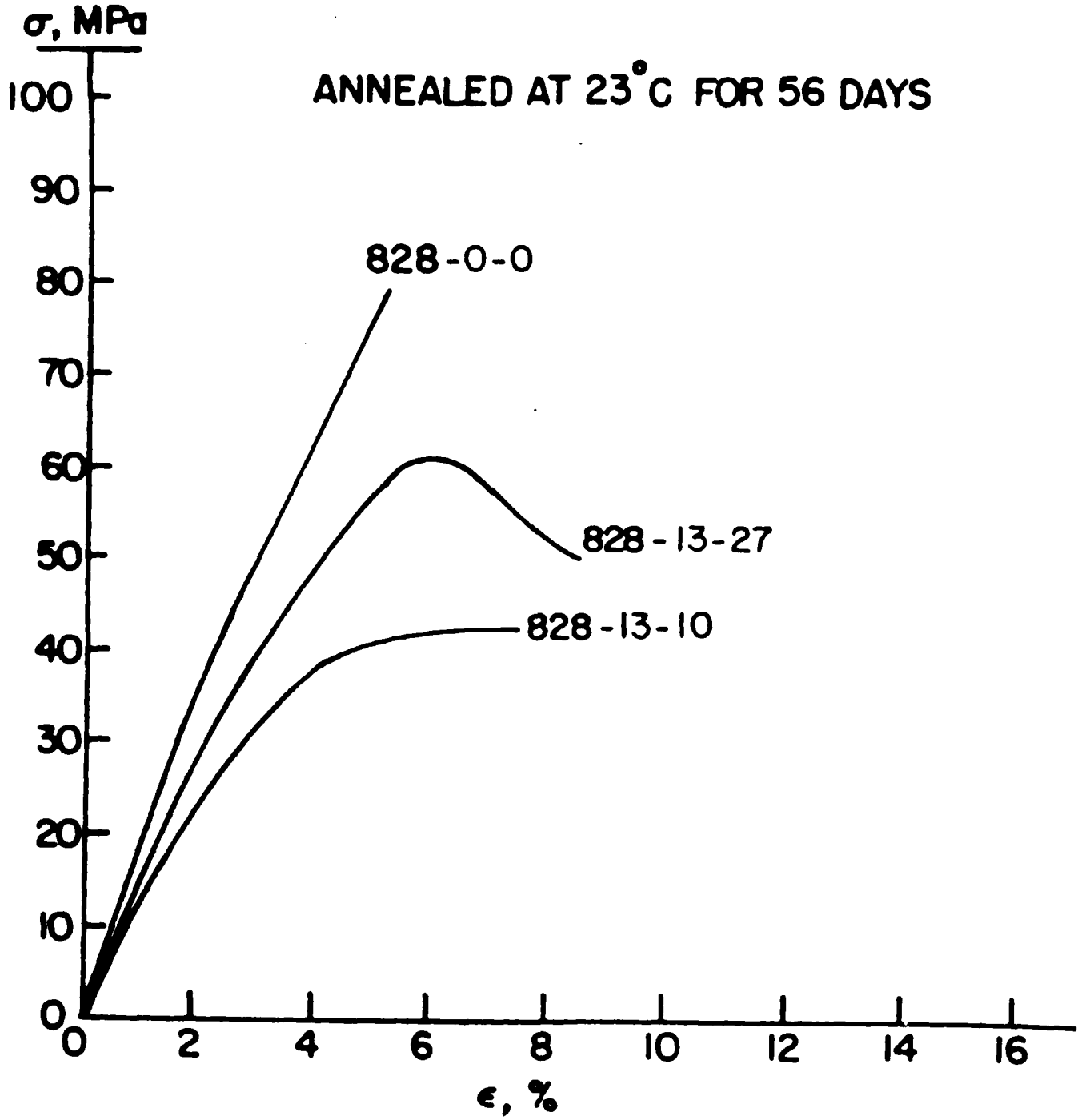
σ, MPa
ANNEALED AT 23°C FOR 56 DAYS
100
90
80
70
60
50
40
30
20
10
0
828-0-0
828-13-27
828-13-10
0
2
4
6
8
10
12
14
16
ε, %

Figure 22b

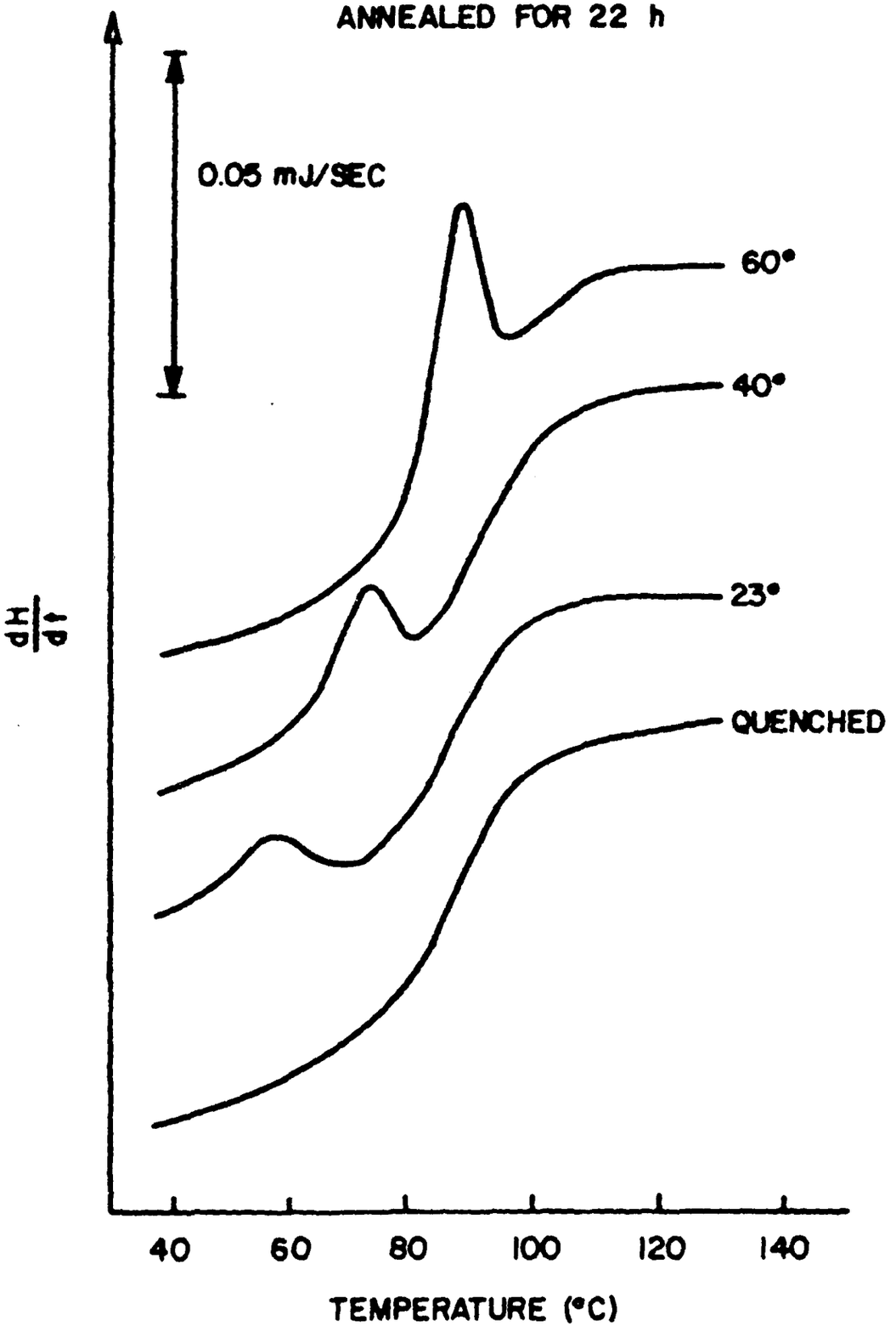
828-0-0
ANNEALED FOR 22 h
0.05 mJ/SEC
60°
40°
23°
QUENCHED
dH/dθ
40
60
80
100
120
140
TEMPERATURE (°C)

Figure 23

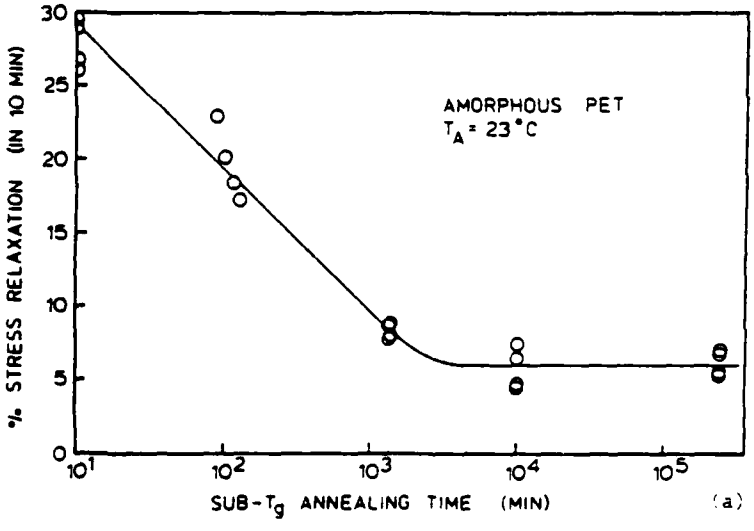
% STRESS RELAXATION (IN 10 MIN)
30
25
20
15
10
5
0
AMORPHOUS PET
T_A = 23 °C
10^1
10^2
10^3
10^4
10^5
SUB-T_g ANNEALING TIME (MIN)
(a)

Figure 24a

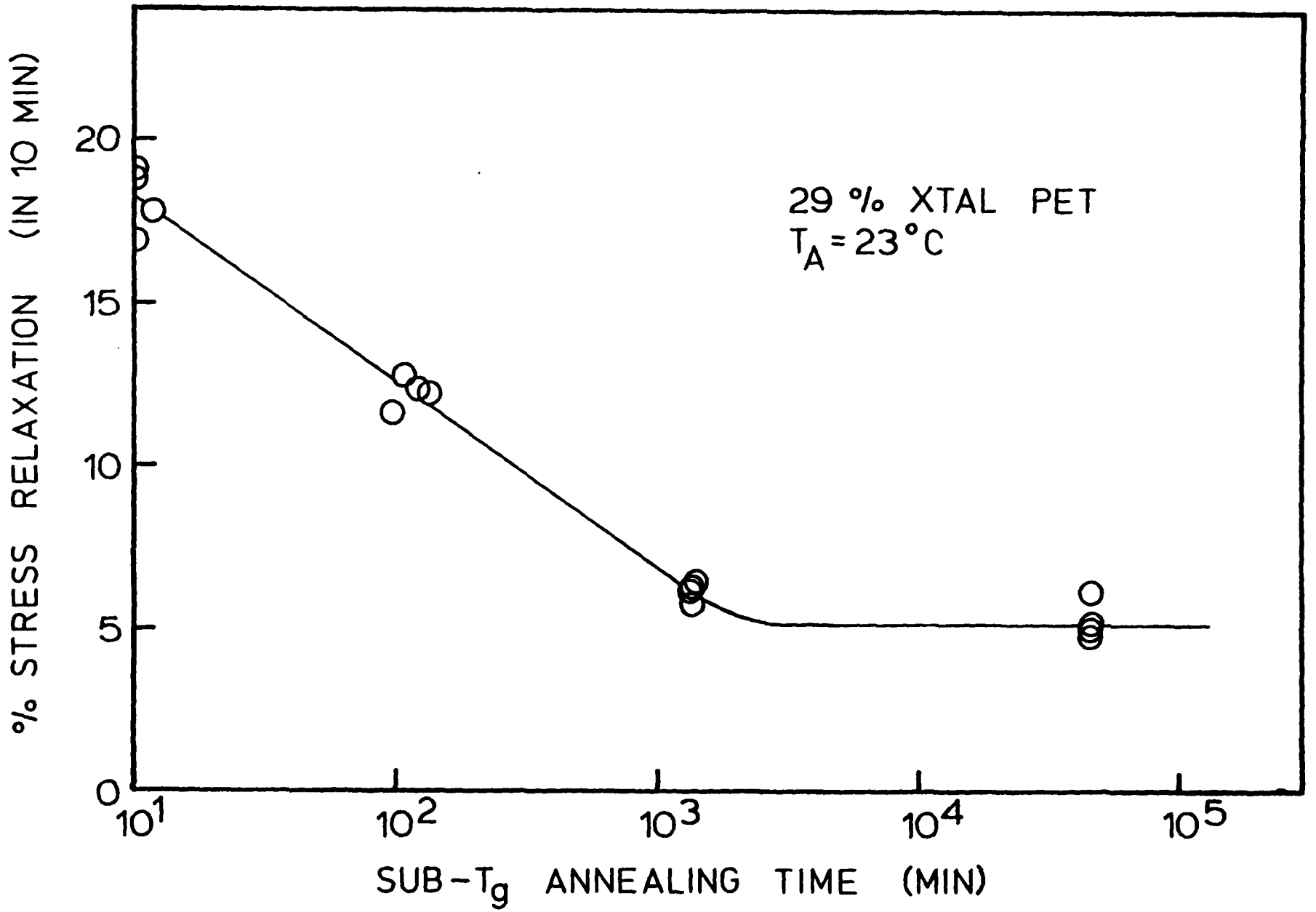
% STRESS RELAXATION (IN 10 MIN)
20
15
10
5
0
29 % XTAL PET
$T_A = 23°C$
10^1
10^2
10^3
10^4
10^5
SUB-T_g ANNEALING TIME (MIN)

Figure 24b

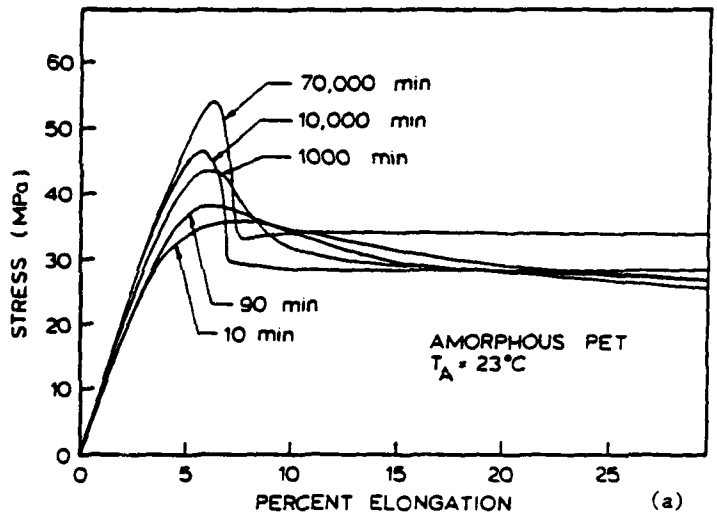

Figure 25a

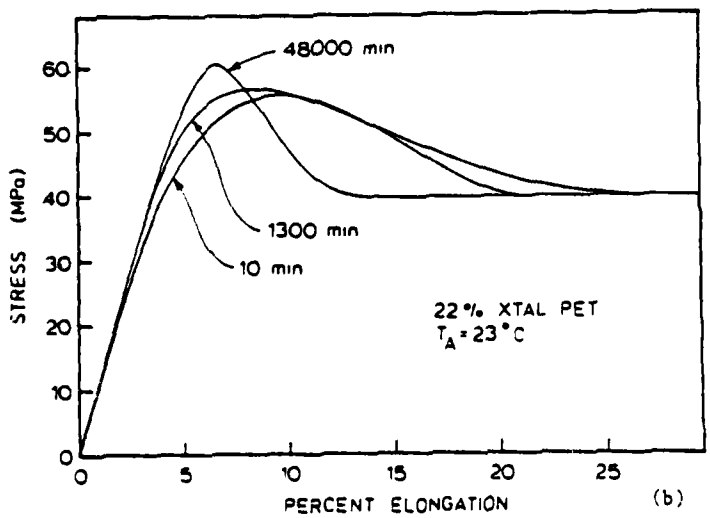

Figure 25b

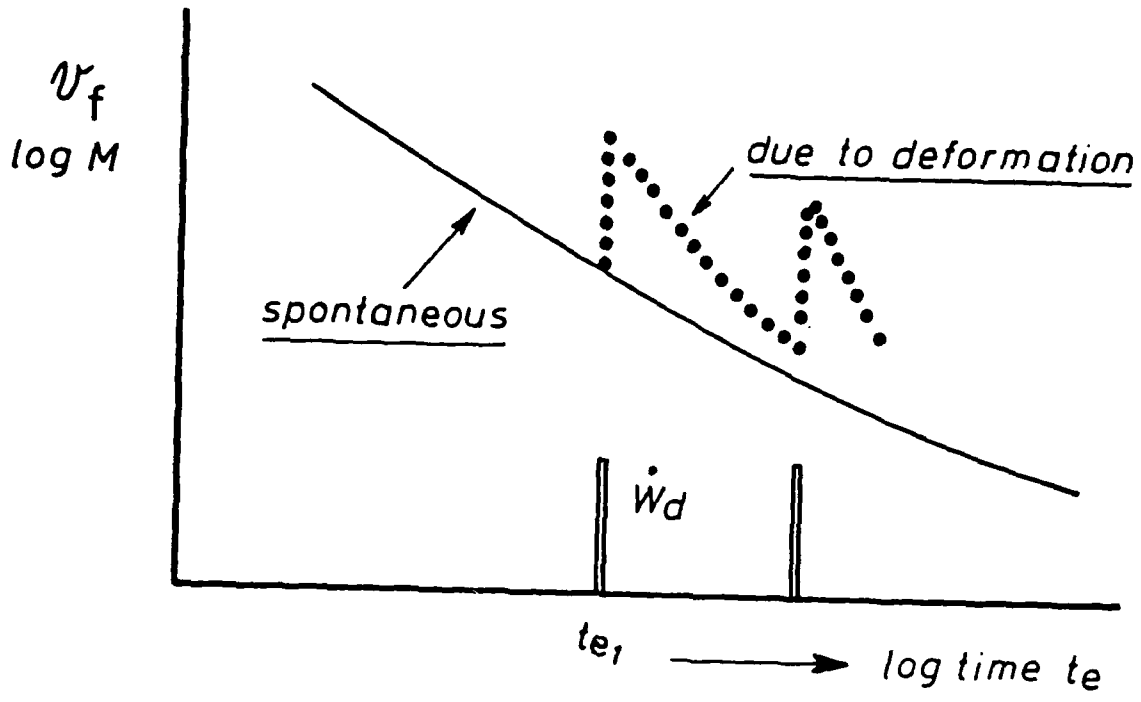

Figure 26

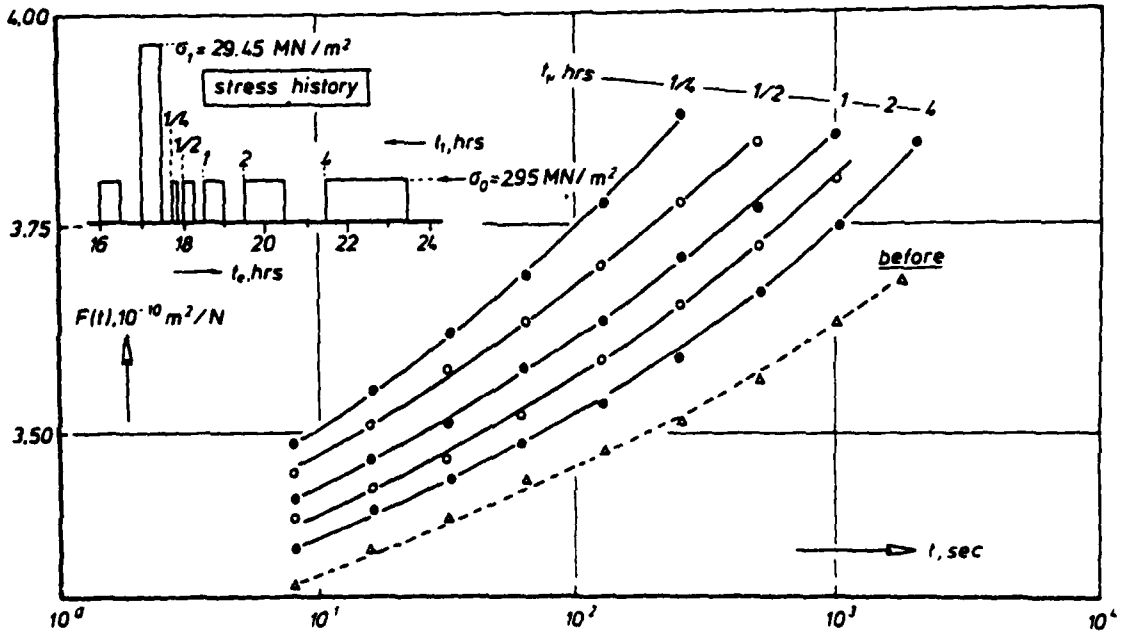

Figure 27

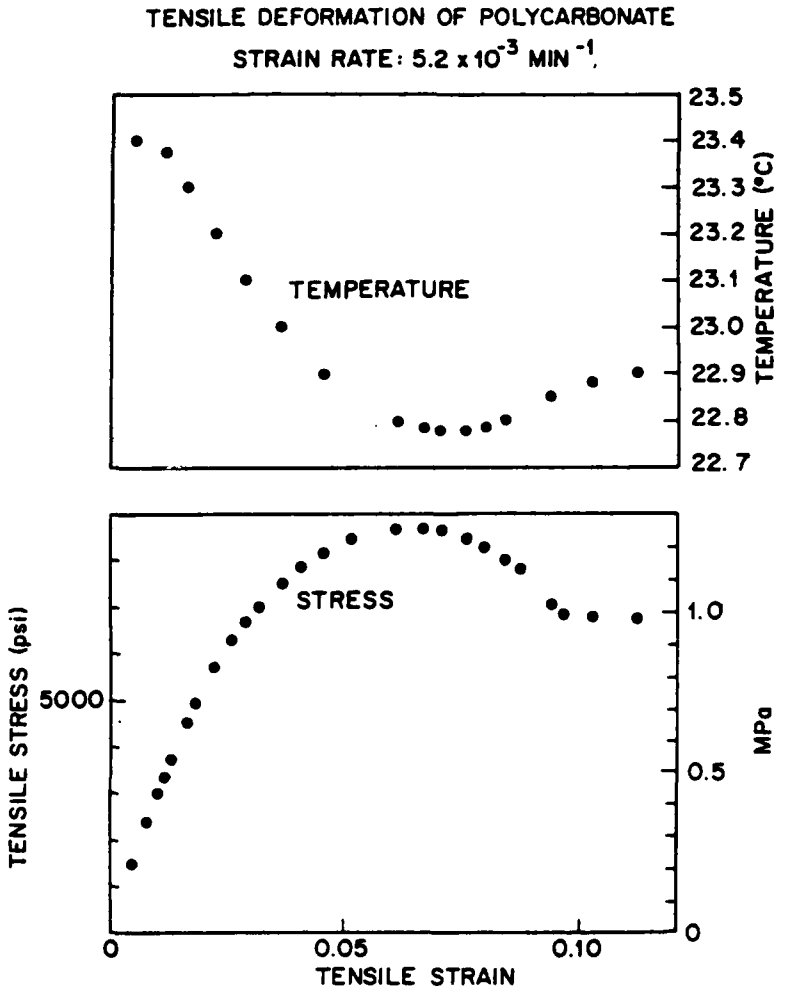
TENSILE DEFORMATION OF POLYCARBONATE
STRAIN RATE: 5.2 x 10^-3 MIN^-1
TEMPERATURE
23.5
23.4
23.3
23.2
23.1
23.0
22.9
22.8
22.7
TEMPERATURE (°C)
STRESS
TENSILE STRESS (psi)
5000
1.0
0.5
0
MPa
0
0.05
0.10
TENSILE STRAIN

Figure 28

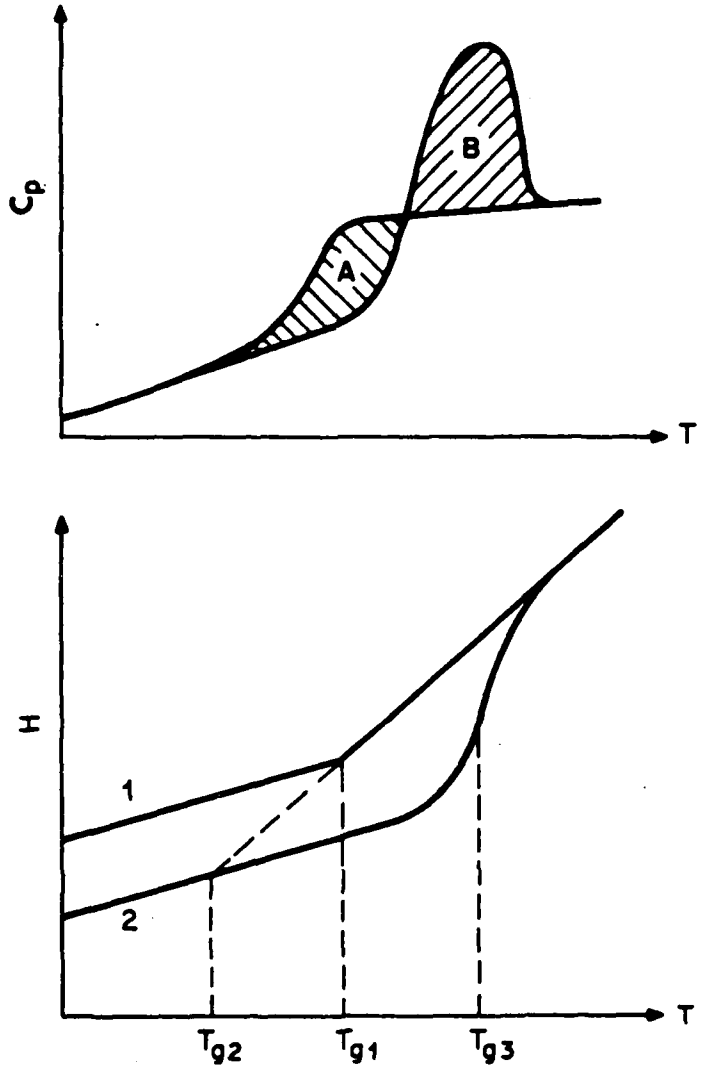

Figure 29

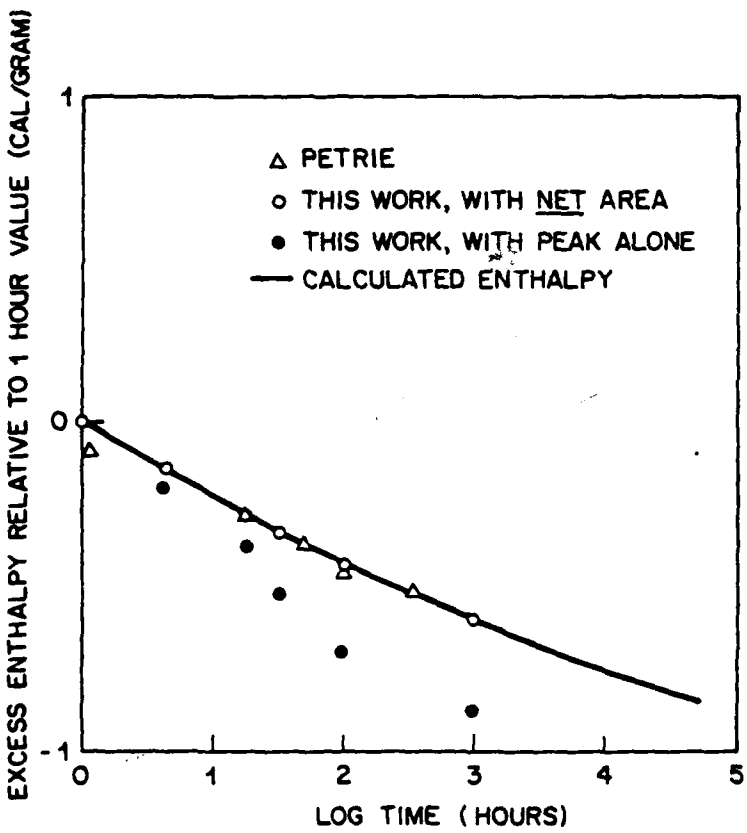
EXCESS ENTHALPY RELATIVE TO 1 HOUR VALUE (CAL/GRAM)
1
0
-1
0
1
2
3
4
5
LOG TIME (HOURS)
△ PETRIE
○ THIS WORK, WITH NET AREA
● THIS WORK, WITH PEAK ALONE
— CALCULATED ENTHALPY

Figure 30

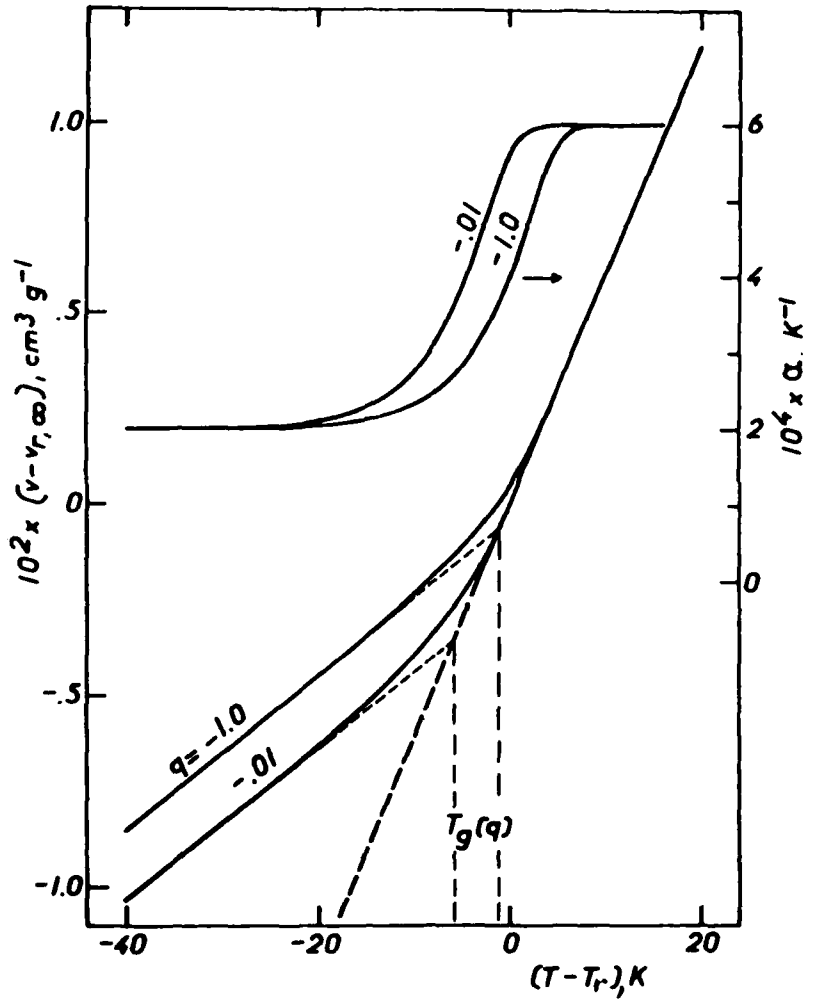

Figure 31a

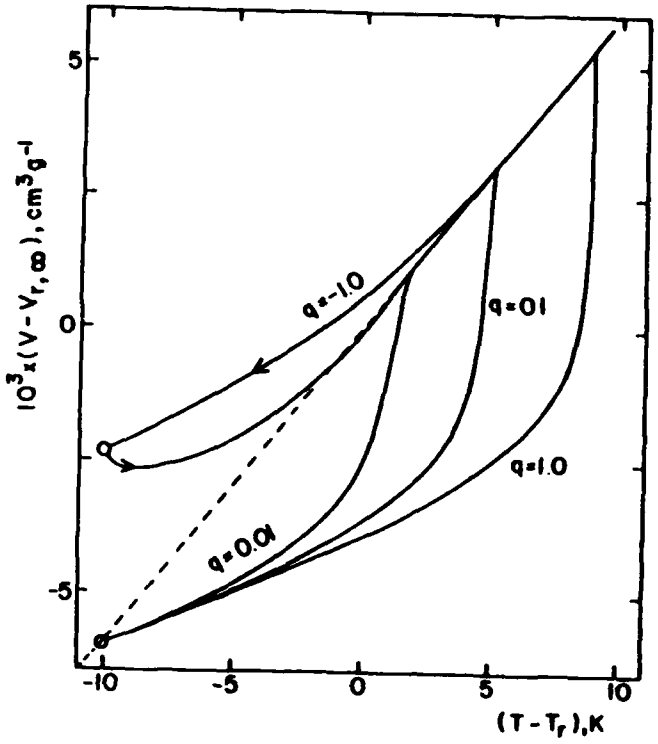

Figure 31b

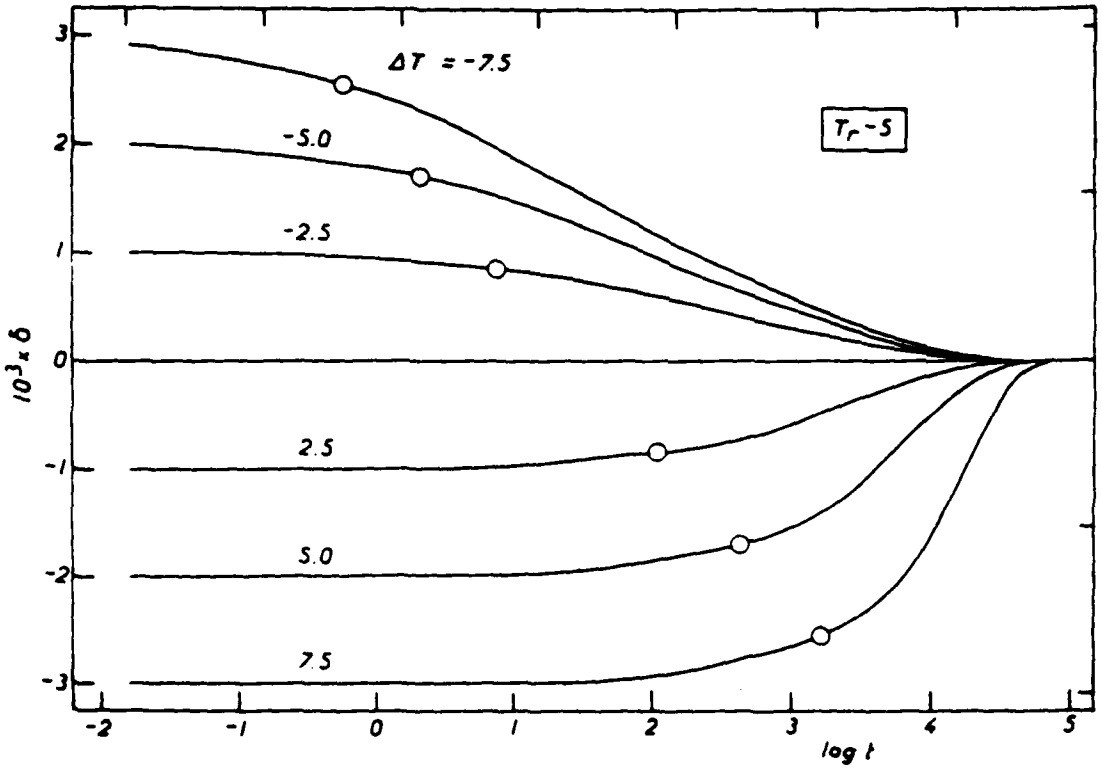

Figure 31c

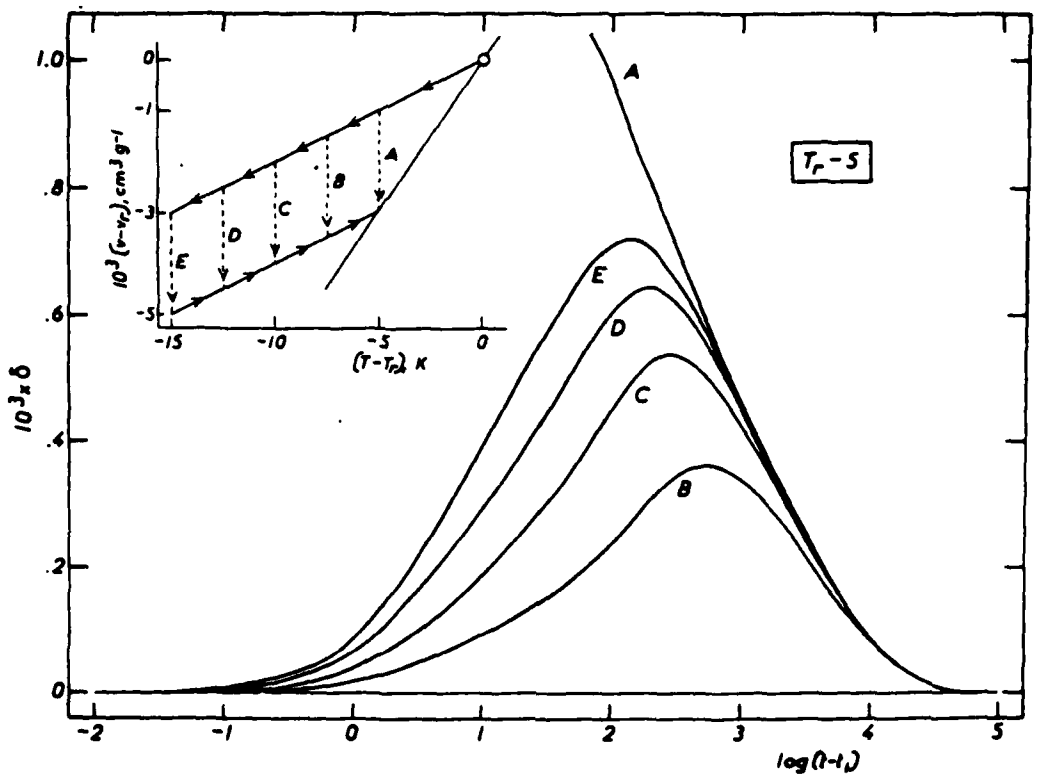
1.0
.8
.6
.4
.2
0
$10^{-3}\times\delta$
-2
-1
0
1
2
3
4
5
log(t-t$_i$)
A
B
C
D
E
T_r - 5
0
-1
-3
-5
$10^3(v-v_r)$, cm^{3}g^{-1}
-15
-10
-5
0
$(T-T_r)_s$ K

Figure 31d

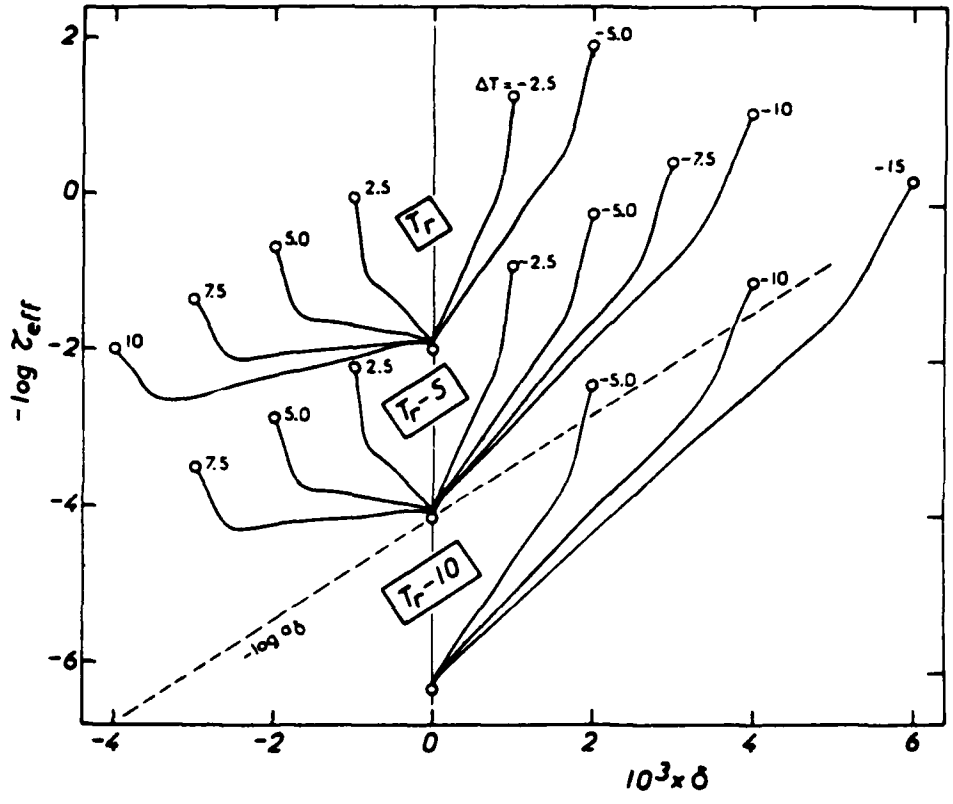
2
0
-2
-4
-6
-4
-2
0
2
4
6
$10^3 \times \delta$
$-\log \tau_{eff}$
T_r
T_r-5
T_r-10
$\Delta T_r = -2.5$
-5.0
-10
-7.5
-15
2.5
5.0
7.5
10
$-\log \omega_b$

Figure 32

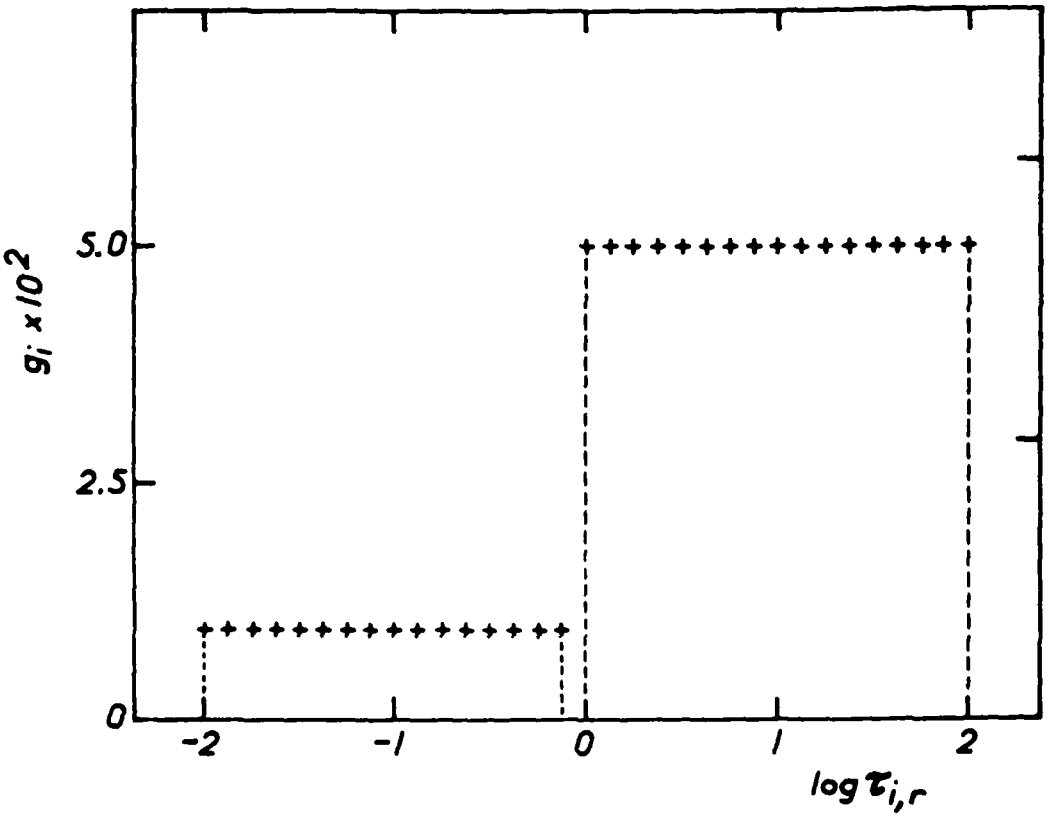

Figure 33

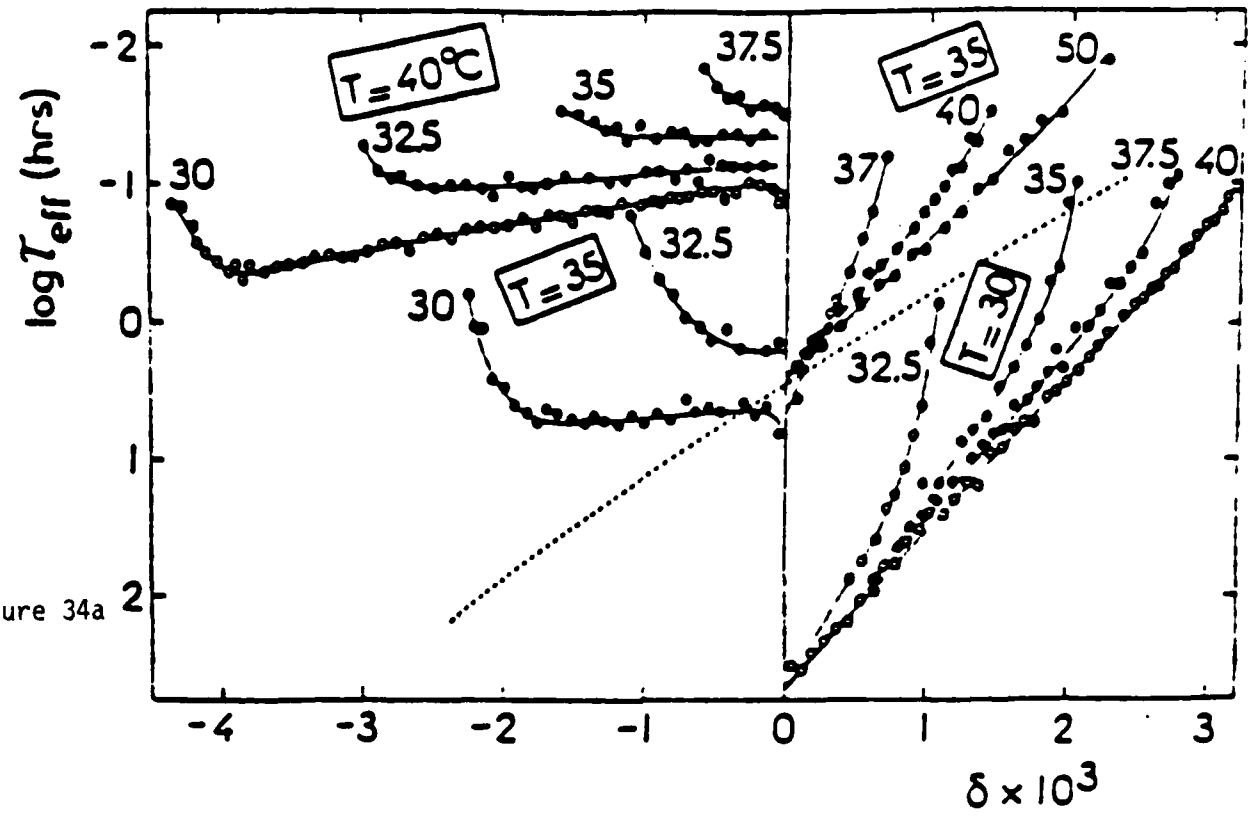

Figure 34a

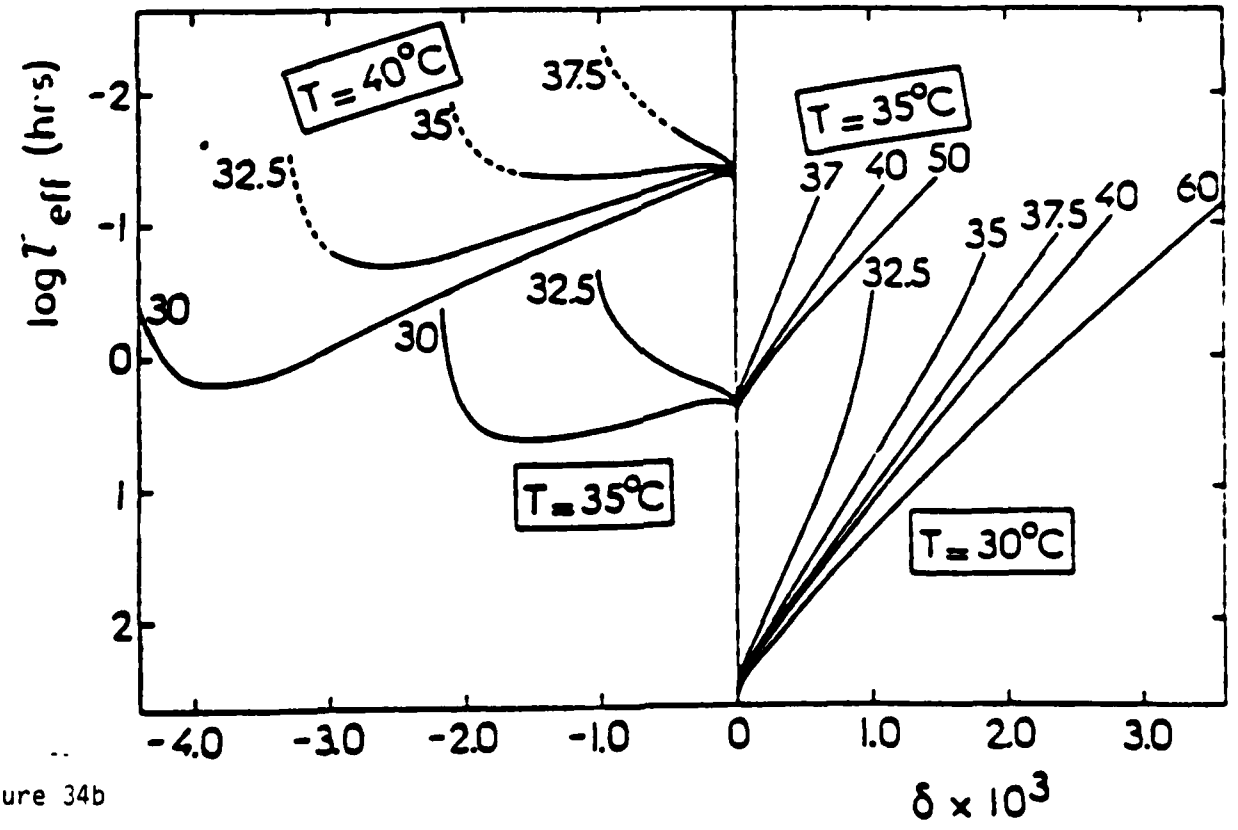

Figure 34b

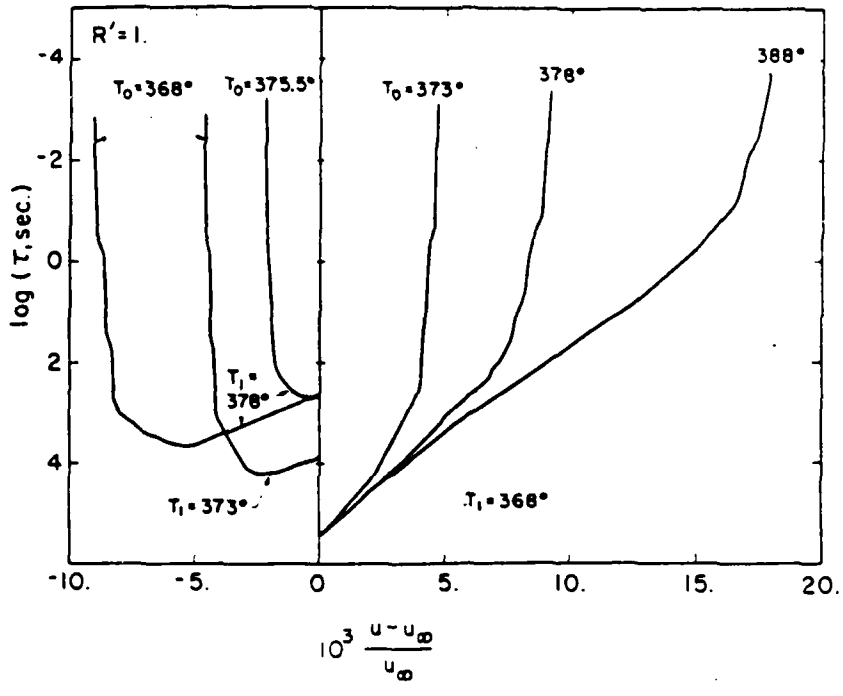
R' = 1.
T_0 = 368°
T_0 = 375.5°
T_0 = 373°
376°
388°
T_1 = 376°
T_1 = 373°
T_1 = 368°
log (τ, sec.)
-4
-2
0
2
4
-10.
-5.
0
5.
10.
15.
20.
$10^3 \frac{u - u_\infty}{u_\infty}$

Figure 35


DATE
ILME